

Journal of **Safety, Health & Environmental Research**

THIS ISSUE

34-42 *QSPR Studies Using Genetic Function Approximation to Predict the Chemical Reactivity of Noncyclic Hydrazines*

43-50 *Incident Analysis of Major Crowd Stampedes*

51-56 *Extracting Kinetic Information Using Power Measurements From Isothermal Calorimeters*

ALSO

•**EDITORIAL:** *Special Issue: Fire & Process Safety*



Journal of Safety, Health & Environmental Research

Managing Editor

Michael Behm
East Carolina University
Greenville, NC

Editorial Board

Sang Choi
University of Wisconsin-Whitewater
Whitewater, WI

Jerry Davis
Auburn University
Auburn, AL

Anthony Veltri
Oregon State University
Corvallis, OR

Qingsheng Wang
Oklahoma State University
Stillwater, OK

ASSE Academics Practice Specialty Administrator

Michael O'Toole
Embry-Riddle Aeronautical University
Daytona, FL

Founding Editor

James Ramsay
Embry-Riddle Aeronautical University
Daytona, FL

Mission: The Journal of Safety, Health and Environmental Research (JSHER) is to peer review theoretical and empirical manuscripts, reviews and editorials devoted to a wide variety of SH&E issues and practices.

Scope: As such, JSHER accepts theoretical and empirical papers committed to concepts, analytical models, strategy, technical tools and observational analyses that enhance the decision-making and operating action capabilities of SH&E practitioners and which provide subject matter for academics. JSHER is an online journal intended to be of interest to SH&E academics and to field practitioners concerned with SH&E science, emergency and disaster preparedness, fire and homeland security, corporate sustainability and resiliency, economic evaluation of SH&E programs or policies, risk-loss control, engineering and other legal aspects of the SH&E field.

control, engineering and other legal aspects of the SH&E field.

Submission Guidelines: Each submission to JSHER will be blind peer-reviewed by at least two reviewers. Submission of a manuscript to JSHER indicates that the effort expressed has not been published previously and that it is not currently under consideration for publication elsewhere.

Manuscripts that are in agreement with JSHER's mission and scope should be crafted carefully and be professionally written. They should be submitted as an attachment within an e-mail message. Specifically, they should:

- be submitted as an MS Word file(s) with no author identifiers;
- be 8 to 20 double-spaced pages with 1" margins all around (approximately 3,000 to 8,000 words, including references, but not including illustrations, tables or figures, which are not included in the text)
- include a separate document with title page indicating the title, co-authors and the person to whom correspondence should be directed, including that person's name, title, employer, phone number, fax number, e-mail address and a short (50-word) bio-sketch of each author indicating at least the author's current position, highest degrees earned and professional certifications earned;
- include an abstract of no more than 200 words, which states briefly the purpose of the research, the principal results and major conclusions, including a short list of key words;
- include a reference section at the end of the manuscript, using APA style to cite and document sources;
- have the pages numbered consecutively and new paragraphs clearly indicated;
- be sure that facts and figures are documented and acknowledged;
- present tables and figure legends on separate pages at the end of the manuscript, but indicate where in the manuscript the table or figure should go;
- make sure that graphics, such as figures and photos, are submitted as separate files and are not embedded in the article text;
- for empirical research, at a minimum, the text should include an introduction, methods, results and discussion sections in the main text;
- for all submission types, section headers, which describe the main content of that portion of the manuscript, are advisable.

Copyright: Authors are requested to transfer copyright to the publisher and submit a copyright agreement form.

All submissions should be sent to:

Michael Behm, Ph.D., CSP
Managing Editor
Associate Professor, Occupational Safety
East Carolina University
231 Slay Hall
Greenville, NC 27858
Phone: (252) 328-9674
behmm@ecu.edu



Special Issue: Fire & Process Safety

With the economy developing forward, technologies are contributing enormously to the quality of our life into the 21st century. Technological advances in chemical, petrochemical and oil and gas areas have brought ever-increasing sophistication of processes and/or systems. These advanced processes pose a severe challenge to current industries as they need to prevent, mitigate and control more potential hazards to achieve cost effectiveness. Fire and process safety has come a long way since the beginning of the 20th century. The safety issue is always considered as an essential part of the industry that needs continual improvement. However, various accidents are still happening and causing tremendous losses of life and property. Keeping in view the importance of fire and process safety, the *Journal of Safety, Health and Environmental Research's* (JSHER) editorial board decided to release a special issue on this topic. After a thorough review process, three papers were selected.

The first paper is "QSPR Studies Using Genetic Function Approximation to Predict the Chemical Reactivity of Noncyclic Hydrazines" by Carlos Espindola-Calderon, Suhani J. Patel, Ammar Alkhalwaldeh, Yuan Lu and M. Sam Mannan from Texas A&M University, College Station, TX, USA. In this work, predictive models using the Quantitative Structure Property Relationship (QSPR) were developed to estimate the chemical reactivity-related properties for noncyclic hydrazines. QSPR models can be used to predict calorimetric experimental data, such as onset temperature and heat of decomposition, using entities derived from the molecular structure for a set of 32 reactive noncyclic hydrazines.

The second paper, "Incident Analysis of Major Crowd Stampedes" by Jacques Albert, Qingsheng Wang, Tingguang Ma and Michael Larranaga, is from Oklahoma State University, Stillwater, OK, USA. This paper developed a list of major crowd stampede incidents. Several factors affecting crowd stampedes were identified and analyzed based on the principles of crowd movement, rumor and panic. It was found that the most significant variable in intense stampede initiations is the social environment in which the crowd exists. The study also indicated that rumor and panic go hand-in-hand in uncertain and ambiguous situations. This work could provide insights into emergency response management of future crowd stampede incidents.

The third paper, "Extracting Kinetic Information Using Power Measurements From Isothermal Calorimeters" by Subramanya Nayak, M. Sam Mannan and Simon Waldram, is original work from Texas A&M University at Qatar, Doha, Qatar. In this paper, the application of the grey prediction model was investigated for failure prognostics of electronics.

The authors demonstrated that both the heat of reaction and kinetic constants of a single chemical reaction can be estimated from a temporal power measurement derived from an isothermal reaction calorimeter. Appropriate mathematical models were developed to extract kinetic information. The derived equations were applied to the hydrolysis reaction of acetic anhydride to estimate enthalpy of reaction, kinetic constants and activation energy.

Finally, I would like to take this opportunity to thank all of the authors and reviewers for extending their cooperation in revising and preparing these papers. Special thanks go to Michael Behm, Ph.D., JSHER managing editor, for guiding me to make this special issue possible. ☺

Qingsheng Wang, Ph.D.

Qingsheng Wang, Ph.D., is assistant professor in the Department of Fire Protection and Safety and the Department of Chemical Engineering at Oklahoma State University, which he joined in 2010. He holds a doctorate in Chemical Engineering from Texas A&M University with an emphasis in Process Safety. He has worked for Shell as technical safety engineer in Houston, TX. Wang is also faculty Fellow at Mary Kay O'Connor Process Safety Center in the Artie McFerrin Department of Chemical Engineering at Texas A&M University. Wang is an active member of ASSE, American Institute for Chemical Engineers, American Chemical Society and American Society for Engineering Education. He is the author of 24 peer-reviewed journal papers and the invited reviewer for more than 20 international journals, such as *AICHE Journal*, *Journal of Hazardous Materials*, *Safety Science* and *Fire Safety Journal*. His research has been in the fields of process safety and fire safety engineering. He can be reached at qingsheng.wang@okstate.edu.

QSPR Studies Using Genetic Function Approximation to Predict the Chemical Reactivity of Noncyclic Hydrazines

Carlos A. Espindola-Calderon, Suhani J. Patel, Ammar Alkhalwaldeh, Yuan Lu and M. Sam Mannan

Abstract

Estimating thermal stability of chemical components using computational methods provides a reliable and useful means to minimize the number of experiments needed and to advance an alternative to performing experiments on nonstable chemicals, hence providing a safer methodology of attaining the needed data.

In this work, predictive models using the Quantitative Structure Property Relationship (QSPR) were developed to estimate the chemical reactivity related properties for noncyclic hydrazines. QSPR models can be used to predict calorimetric experimental data, such as onset temperature and heat of decomposition, using entities derived from the molecular structure for a set of 32 reactive noncyclic hydrazines. Molecular descriptors that are strongly dependant on geometry were calculated after molecular geometry optimization, such as ϵ_{HOMO} , ϵ_{LUMO} , dipole moment (DM), total energy and others. These descriptors describe the thermal stability of hydrazines more effectively. Genetic function approximation analysis was used to predict the final model for each property. The reliability of the QSPR model was assessed by statistical parameters, such as R^2 , $R^2_{(CV)}$ and F value, which are 0.895, 0.833 and 29.201 for onset temperature and 0.978, 0.660 and 95.133 for heat of decomposition.

Keywords

Quantitative Structure-Property Relationship (QSPR), hydrazines, Genetic Function Approximation (GFA), thermal stability, onset temperature, heat of decomposition

Introduction

Assessment of the thermal stability of materials is important for the design and operation of any hazardous process in the chemical industry (Aldeeb, et al., 2002). Such information can be used to create guidelines for handling, storage and transport of chemical compounds and to avoid violent reactions that can lead to catastrophic events resulting from a sudden release of energy (CCPS, 1995), such as the incident at Savannah River or Toms-7, where hydrazines and nitric acid mixtures were used during recycling of spent fuel (Miyake, et al., 2005).

Therefore, it is necessary to understand the danger associated with each reagent and the conditions under which the hazard can be propagated. Previous research (Ando, et al., 1991; Saraf, et al., 2003c) showed that it is possible to predict

and classify the thermal hazards of reactive chemicals in terms of a sensitivity measure (i.e., Onset Temperature, T_o) and a severity measure (i.e., heat of decomposition, $-\Delta H$) (Ando, et al., 1991). T_o and $-\Delta H$ values have been determined for many reactive chemicals using Differential Scanning Calorimetry (DSC) experiments to characterize the thermal stability of reactive chemicals. Nevertheless, these experiments are limited to a few number of compounds because many substances are highly unstable and cannot be measured safely (Ando, et al., 1991). Hence, much attention has been paid recently to using computational methods to predict these properties based on limited experimental data (Saraf, et al., 2003a).

Sensitivity and severity of hazardous materials strongly depend on the chemical structure of a substance (Grewer, 1991). Thus, an emerging property prediction technique, Quantitative Structure Property Relationship (QSPR), becomes an attractive alternative to extend actual calorimetric data to a larger set of compounds using computational chemistry to describe molecular and electronic structure. QSPR technique is used to predict physical or chemical properties by using entities known as molecular descriptors. These descriptors are values calculated from the 2D or 3D representation of a molecular structure. Several QSPR studies have been developed not only for thermal analysis (Fayet, et al., 2009; Lu, et al., 2011), but also to predict other physicochemical properties related to hazardous materials, such as flash points (Patel, 2009), autoignition temperature (Pan, et al., 2009), explosivity limits (Gharagheizi, 2009), etc.

Recently, efforts have been focused toward certain materi-

Carlos A. Espindola-Calderon is a graduate student in chemical engineering at Texas A&M University.

Suhani J. Patel, Ph.D., was a graduate student of chemical engineering at Texas A&M University and is now working at Shell in Houston, TX.

Ammar Alkhalwaldeh, Ph.D., is a research scientist in the Mary Kay O'Connor Process Safety Center at Texas A&M University. He can be contacted at toammar@mail.che.tamu.edu.

Yuan Lu, Ph.D., was a graduate student in chemical engineering at Texas A&M University and is now working at OXY in Houston, TX.

M. Sam Mannan, Ph.D., is regents professor of chemical engineering and director of the Mary Kay O'Connor Process Safety Center at Texas A&M University. He can be contacted at mannan@tamu.edu.

als considered to be more hazardous, such as nitro compounds (Fayet, et al., 2009) and peroxides (Lu, et al., 2011); however, it is also necessary to know more about the moderately hazardous material, which under different conditions can possibly change their reactive behavior dramatically. In this work, the type of moderately hazardous chemicals evaluated is the family of noncyclic hydrazines.

Hydrazines, which are flammable, highly toxic and relatively unstable materials (usually handled in solutions to mitigate that effect), are widely used in industry and have the potential to cause serious hazards if not handled properly. They are strong reducing agents, and their oxidation reaction is highly exothermic (148.6 kcal/mol). They can exothermally decompose or explode in the presence of platinum (at 86° F in the presence of oxygen) or some oxides (iron, copper, barium and others). In addition, they are not compatible with ammonia and some organic compounds, and they are shock-sensitive materials (Schirmann & Bourdauducq, 2002; NCBI PubChem, Chemical product info-chemindustry.ru).

More than 260,000 tons of hydrazines are produced annually, and applications in which they are used include foaming agents, precursors to polymerization catalysts, rocket fuels, pharmaceuticals, agents to reduce dissolved oxygen in industrial boilers and many others. Developing predictive methods for the reactivity of such materials is of great importance (Schirmann & Bourdauducq, 2002; NCBI PubChem, Chemical product info-chemindustry.ru).

In this study, QSPR methodology, along with Genetic Function Approximation (GFA), was used to correlate onset temperature and heat of decomposition with molecular descriptors. It involved combination of Friedman's multivariate adaptive regression splines (MARS) algorithm with Holland's genetic algorithm (Rogers & Hopfinger, 1994). The GFA algorithm generates different QSPR models from various descriptors calculated using Material Studio 5.0 software (Accelrys Software Inc.) (Accelrys, 2006b).

Molecular descriptors are entities that can be calculated from information held within the symbolic representation of a molecule. During QSPR analysis, molecular optimization was performed to make the geometry more stable for each molecule; thereafter molecular descriptors affecting the kinetic and exothermic decomposition were calculated. Several models were built to find a reasonable and more accurate correlation.

Methodology

Input Data

The experimental calorimetric data set for noncyclic hydrazines was collected from Differential Scanning Calorimetry (DSC) experiments reported in literature (Ando, et al., 1991). This dataset is composed of 32 substances (shown in Table 4).

One of the most important steps is the data selection because experimental conditions have strong influence on the studied properties. For this reason, all experimental values used must be obtained using the same procedure under identical conditions. These sets of values were obtained with an aluminum pinhole cell and argon at 3.5 MPa.

To verify the quality of the data collected and to ensure the reliability of the model, a preliminary analysis was performed where the distributions of each variable were plotted, verifying that the data distribution had the same behavior as a normal distribution. This is a requirement for multivariate analysis.

Geometry Optimization

Additionally, 2D structures for corresponding molecules were collected from PubChem database (NCBI). This format does not provide sufficient information to calculate all descriptors; therefore, it is necessary to optimize the geometry to find an equilibrium-state, low-energy structure of the molecule. For each molecule of the data set, 3D geometry optimization was performed using Gaussian 03 software package (Frisch, et al., 2003) with the B3LYP, density functional theory level and the 6-31G basis set. This is necessary because the values of several descriptors can strongly depend on orientation of the atoms in the molecule.

Molecular Descriptors

Molecular descriptors were calculated after geometry optimization and chosen depending on the property to be correlated. In this work, descriptors that were expected to correlate with thermal stability were selected as follows.

- Eigen value of highest occupied molecular orbital (ϵ_{HOMO}) is the energy of the highest level containing electrons in the molecule. A molecule with higher ϵ_{HOMO} value is able to donate electrons more easily, thus it is relatively more reactive than a molecule with lower ϵ_{HOMO} value (Saraf, et al., 2003b). The negative of ϵ_{HOMO} is also known as ionization potential (IP) (Fayet, et al., 2009).

- Eigen value of lowest unoccupied molecular orbital (ϵ_{LUMO}) is the energy of lowest level in the molecule that does not contain electrons. A molecule with lower ϵ_{LUMO} value is able to accept electrons more easily than a molecule with higher ϵ_{LUMO} value (Saraf, et al., 2003b). The negative of ϵ_{LUMO} is also known as electron affinity (EA) (Fayet, et al., 2009).

- Highest positive charge (HPC) and lowest negative charge (LNC) are the driving force for electrostatic interactions. The electron densities on a particular atom characterize the possible orientation of the chemical interactions and can be considered as directional reactivity indices (Karelson, et al., 1996).

- Nitrogen-nitrogen (NN) bond distance is a kinetic descriptor because it represents the minimum energy required to break the NN bond and thereafter initiate the reaction.

- Delocalizability (Sr) is an index of the reactivity of occupied and unoccupied orbitals and is defined as (Karelson, et al., 1996) where ϵ_i is the energy at each level.

$$Sr = \sum_{i=1}^{HOMO} \frac{1}{\epsilon_i} \quad (1)$$

- Dipole moment (DM) can describe the electronic structure and can reflect the global polarity of a molecule.

•Hardness (η), or chemical hardness, is defined as resistance of the chemical potential to any change in the number of electrons (Parr & Pearson, 1983) and is defined as shown in equation 2.

$$\eta = \text{IP} - \text{EA} = \epsilon_{\text{LUMO}} - \epsilon_{\text{HOMO}} \quad (2)$$

•Molecular weight (MW), oxygen balance (OB) and number of hydrazine functional groups (NHG) are constitutional descriptors (Fayet, et al., 2009). These are derived from composition of compound and do not depend on the geometry. According to Shanley and Melhem (1995), the oxygen balance is defined as shown in equation 3.

$$OB = \frac{[-1600(2X + \frac{Y}{2} - Z)]}{MW} \quad (3)$$

Where X is the number of carbon atoms, Y is the number of hydrogen atoms, Z is the number of oxygen atoms and MW is the molecular weight.

•Chemical potential (μ) is the measure of the escaping tendency of electrons from the system and is defined as shown in equation 4.

$$\mu = \frac{\epsilon_{\text{HOMO}} + \epsilon_{\text{LUMO}}}{2} \quad (4)$$

•The electrophilicity index (ω) has been constructed to measure the loss in energy for a maximal electron flow from donor to acceptor (Parr, et al., 1999). This descriptor has been used in the prediction of thermal stability for other functional groups (Fayet, et al., 2009). The ω is defined as shown in equation 5.

$$\omega = \frac{\mu^2}{2\eta} \quad (5)$$

•The mean polarizability (α) is the average of diagonal components of the polarizability matrix, which helps in describing the electronic structure.

$$\alpha = \frac{1}{3}(\alpha_{XX} + \alpha_{YY} + \alpha_{ZZ}) \quad (6)$$

where α_{XX} , α_{YY} and α_{ZZ} are the diagonal components of the polarizability matrix.

•Total energy (TE) of the molecule has been used in different cases and is dependent on the electronic energy of the molecule as well as the repulsion energy between the nuclei.

After having calculated molecular descriptors, a preliminary analysis was performed to identify the descriptors, which were highly correlated. This was done using a correlation matrix, where some descriptors were removed from further analysis according to the value of correlation coefficients. This analysis was done in order to keep the most relevant descriptors only, avoiding multicollinearity in further analysis.

Generation of QSPR Models

QSPR analysis was used to generate the models to correlate onset temperature and heat of decomposition with molecular descriptors. QSPR models were obtained using GFA algorithm, which allows building high-quality predictive models combining genetic algorithms and multivariate adaptive regression splines (Rogers & Hopfinger, 1994). The models took the general form as shown in equation 7 (Shi, et al., 1998).

$$y = f(x) = a_0 + \sum_{i=1}^n a_i B_j(x_i) \quad (7)$$

Where y is the independent variable (property), the values of a_i are coefficients of each term in the equation (calculated by the software); x_i are descriptors included in the model; n is the number of descriptors in the model; $B_j(x_i)$ is a specific function for the corresponding descriptor x_i , which can be a quadratic, logarithmic or even a spline transformation.

The genetic algorithm used to select the coefficients and set of descriptors is as follows (Shi, et al., 1998):

•Initial population of equations is randomly generated, and knot value is randomly initialized. The knot of the spline is a constant, α such that $\langle x - \alpha \rangle$ evaluates to 0 when x is less than α and to $\langle x - \alpha \rangle$ otherwise.

•The models are scored using Friedman's (Friedman lack of fit) measure, using slight variation of the original Lack of Fit (LOF) value as shown in equation 8 (Accelrys, 2006a).

$$LOF = \frac{SSE}{M \left[1 - \lambda \left(\frac{c + d \times p}{M} \right) \right]^2} \quad (8)$$

Where SSE is the sum of square errors, c is the number of terms in the model, d is a scaled smoothing parameter, p is the total number of descriptors contained in all model terms, M is the number of samples in the training set and λ is a safety factor, with the value of 0.99, to ensure that the denominator of expression can never become zero.

The scaled smoothing parameter is related to scaled LOF smoothness parameter α in the equation 9 where c_{max} is the maximum equation length

$$d = \alpha \left(\frac{M - c_{\text{max}}}{c_{\text{max}}} \right) \quad (9)$$

•Once all equations in the population have been scored using the LOF value, the genetic crossover operation is repeatedly performed, and progeny equations are developed combining two parent strings into a new child string (Rogers & Hopfinger, 1994).

•If a duplicate of the resulting model does not already exist in the population, the model with the worst LOF score is replaced by the new child.

Following this method, 50,000 iterations were performed to obtain the QSPR models for onset temperature and heat of decomposition. The final equations generated were validated with the following parameters: (a) R-squared value; (b) R-squared cross validated value; (c) F-value; (d) LOF measured; (e) average absolute deviation; (f) average absolute relative deviation; and (g) average percent bias.

Results & Discussion

Within the initial data analysis, it was necessary to apply various mathematical transformations to change the shape of the distribution of the input data for heat of decomposition, adjusting it to a normal distribution. The best fit for normal distribution was obtained when the logarithmic function was applied to heat of decomposition as shown in Figure 1.

Molecular descriptors were calculated for the 32 molecules of the input set as reported in Tables 1 and 2. Thereafter, the correlation matrix identified the variables strongly correlated between themselves ($R^2 > 0.9$). According to this analysis, μ and α were excluded because they are highly correlated.

QSPR models were developed correlating molecular descriptors with onset temperature and heat of decomposition. Several variables and splines were created by GFA algorithm, increasing the amount of possible variables for the final model, therefore, improving the accuracy of the model. The best models selected for each property

$$T_o = -235.773 \times \text{ramp}(HPC - 0.647) - 31822.774 \times \text{ramp}(NN - 1.411) - 18.771 \times \text{ramp}(OB + 115.344) + 15249.896 \times \text{ramp}(IP - 0.225) - 0.079 \times \text{ramp}(-965.601 - TE) + 0.164 \times (\text{ramp}(OB + 139.815))^2 - 158402.052 \times (\text{ramp}(IP - 0.203))^2 + 270.822 \dots (10)$$

$$\log(-\Delta H) = -21.727 \times (NN.IP) - 1 \times E - 09 \times TE^3 - 2.623 \times E - 06 \times (TE^2 \times HPC) + 0.244 \times (HPC.DM.NHG) + 7.082 \times E - 04 \times (NN.DM.OB) + 344.398 \times \text{ramp}(NN - 1.411) - 58.094 \times \text{ramp}(\omega - 0.0579) + 193.815 \times \text{ramp}(\omega - 0.0731) - 117.051 \times \text{ramp}(\omega - 0.0854) - 36.421 \times \text{ramp}(0.252 - IP) + 13.505 \dots (11)$$

according to statistical parameters mentioned in Section 0, are presented in equations 10 and 11. Equation 10 has a total of 5 molecular descriptors, and equation 11 has 8 descriptors.

In equations 10 and 11, ramp expression means the application of a first-order spline function. Also, instead of using ϵ_{HOMO} and ϵ_{LUMO} , nonnegative values, i.e., IP and EA, were substituted correspondingly. Table 3 shows the statistical parameters of QSPR models using GFA.

The calculated values for the onset temperature and heat of decomposition using the equations obtained are shown in Table 4, and the experimental and calculated values have been plotted in Figures 2 and 3.

To verify the similarity between experimental and predicted data, a statistical evaluation of error and deviation between

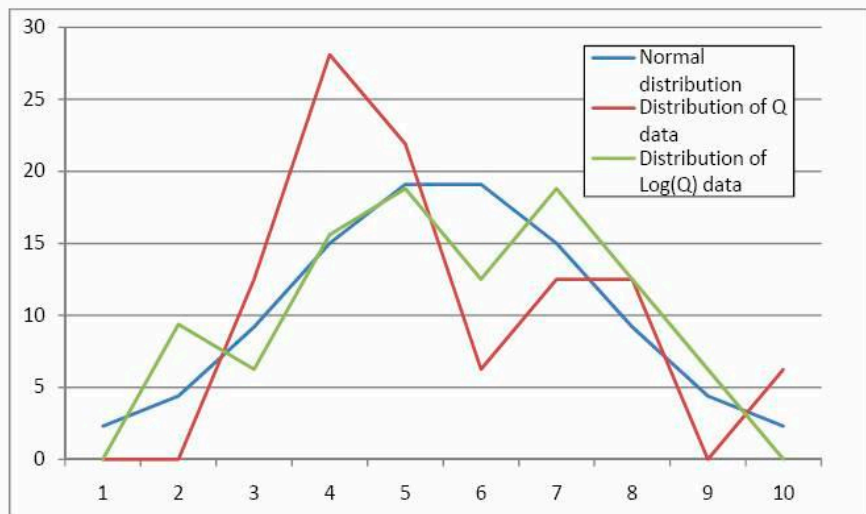


Figure 1. Distribution of Q and Log(Q) data.

predicted and experimental values was performed. It measures the spread of data considering the effect of total number of data, using equations 12, 13 and 14 (below). The values obtained are reported in Table 5.

Statistical parameters (R^2 , R^2_{cv} and F value) of obtained QSPR models using GFA algorithm (Table 2) show high accuracy between experimental data and predicted data (R^2 and $R^2_{cv} > 0.6$) for 32 molecules of training set. The statistic validity of the final model is verified by the cross-validation test, which is meant to examine whether the correlation model is just a mathematic fitting or if it truly represents the relationship. The cross-validation test result, R^2_{cv} , indicates the predictive power of the correlation model. According to the R^2_{cv} value presented in the paper, both onset temperature and heat of reaction prediction models show reasonable predictive power.

The use of such models is most suited for preliminary estimation of the thermal stability of noncyclic hydrazines. This provides very useful screening capabilities through which materials can be classified based on their hazardous potential. Screened materials that meet certain criteria are then investigated further using other techniques and tools. Since the data collected are not enough to obtain a robust correlation, it is also necessary to validate and test each correlation with other calorimetric data sets obtained at the same conditions of training set.

Conclusions

Assessment of the thermal stability can be carried out using computational methods for potential application in preliminary analysis of reactive chemicals before performing calori-

$$\text{Average absolute deviation} = \frac{1}{n} \sum_{i=1}^n |X_{\text{experimental}} - X_{\text{predicted}}| \quad (12)$$

$$\text{Average absolute relative deviation} = \frac{1}{n} \sum_{i=1}^n \left| \frac{X_{\text{experimental}} - X_{\text{predicted}}}{X_{\text{experimental}}} \right| \quad (13)$$

$$\text{Average percent bias} = \frac{1}{n} \sum_{i=1}^n \frac{X_{\text{experimental}} - X_{\text{predicted}}}{X_{\text{experimental}}} \quad (14)$$

Table 1. Data set of noncyclic hydrazines and molecular descriptors calculated (Set 1). Acronyms listed at end of paper.

Chemical Name	EHOMO (a.u.)	ELUMO (a.u.)	HPC	LNC	NN (Å)	Sr	DM	OB	MW (g/mol)
Adipodihydrazide	-0.250	0.014	0.757	-0.930	1.409	79.828	2.689	-156.142	174.201
4-Amino-3-hydrazino-5-mercapto-1,2,4-triazole	-0.204	-0.006	0.482	-1.089	1.400	57.178	3.682	-76.621	146.174
p- Aminobenzoyl hydrazide	-0.206	-0.021	0.640	-1.080	1.411	67.714	4.986	-185.227	151.166
Benzenesulfohydrazide	-0.261	-0.041	0.800	-0.690	1.415	67.957	5.757	-130.078	172.205
Benzoylhydrazine	-0.252	-0.042	0.543	-0.933	1.410	59.513	2.760	-199.778	136.151
Biscyclohexanone oxalylidihydrazine	-0.241	-0.050	0.415	-0.555	1.389	122.994	10.248	-212.682	278.350
Carbohydrazide	-0.251	0.050	0.637	-0.860	1.405	41.305	1.919	-71.044	90.085
1,2-Diformylhydrazine	-0.248	-0.024	0.415	-0.508	1.397	107.091	0.005	-72.673	88.065
1,1-Diphenyl-2-picrylhydrazine	-0.217	-0.142	0.755	-0.498	1.388	79.630	5.839	-147.726	395.326
1,4-Diphenylsemicarbazide	-0.205	-0.005	0.898	-0.908	1.388	151.859	3.521	-221.771	227.262
1,5- Diphenylcarbazide	-0.202	-0.006	0.837	-0.544	1.386	99.521	3.601	-211.329	242.276
2-Hydrazinobenzothiazole	-0.214	-0.026	0.437	-0.986	1.406	65.867	0.158	-169.476	165.216
2-Hydroxy-3-naphthoic acid hydrazide	-0.210	-0.068	0.735	-0.941	1.409	85.539	3.529	-197.815	202.209
2-Hydroxyethylhydrazine	-0.215	0.068	0.473	-0.874	1.411	38.710	2.463	-147.179	76.098
Isonicotinic acid hydrazide	-0.256	-0.065	0.590	-0.940	1.409	57.961	2.264	-169.171	137.139
Isophthaloyldihydrazide	-0.256	-0.059	0.682	-0.930	1.410	83.128	4.763	-156.547	194.191
m-Nitrobenzhydrazide	-0.271	-0.114	0.741	-0.911	1.409	72.273	6.273	-128.072	181.149
Malonyl dihydrazide	-0.250	-0.011	0.757	-0.978	1.412	57.759	2.555	-96.881	132.121
Nicotinohydrazide	-0.250	-0.058	0.661	-0.934	1.409	58.115	4.107	-169.171	137.139
4-Nitrophenylhydrazine	-0.225	-0.083	0.688	-0.765	1.386	64.388	9.466	-141.049	153.139
o-nitrobenzhydrazide	-0.261	-0.116	0.616	-0.895	1.406	72.817	5.077	-128.072	181.149
o-Nitrophenylhydrazine	-0.223	-0.094	0.805	-0.893	1.399	64.061	5.123	-141.049	153.139
Oxalic dihydrazide	-0.255	-0.048	0.448	-0.948	1.409	50.087	3.976	-67.742	118.095
p-Nitrobenzhydrazide	-0.273	-0.120	0.710	-0.932	1.409	71.948	4.149	-128.072	181.149
Phenylazoformic acid-2-phenylhydrazide	-0.205	-0.103	1.113	-0.627	1.385	102.746	4.227	-206.443	240.261
Phenylhydrazine	-0.186	0.019	0.383	-0.826	1.382	51.331	2.870	-236.728	108.141
Phenylhydrazine-4-sulfonic acid	-0.229	-0.071	0.773	-0.751	1.386	74.299	8.858	-115.425	180.203
1-Phenylsemicarbazide	-0.201	0.010	0.856	-1.110	1.389	67.468	4.052	-185.227	151.166
Salicyl hydrazide	-0.233	-0.027	0.625	-0.915	1.409	66.118	3.612	-168.254	152.151
Thiocarbohydrazide	-0.200	0.005	0.436	-1.046	1.404	43.823	5.383	-75.365	106.150
2-Thiophenecarboxylic hydrazide	-0.251	-0.058	0.647	-0.922	1.408	55.655	3.575	-135.041	142.179
2,4,5-Trichlorobenzenesulfonyl hydrazide	-0.247	-0.117	0.664	-0.551	1.322	88.111	5.061	-72.585	275.540

Table 2. Data set of noncyclic hydrazines and molecular descriptors calculated (Set 2). Acronyms listed at end of paper.

Chemical Name	NHG	η (a.u.)	μ (a.u.)	ω (a.u.)	α_{xx} (\AA^3)	α_{yy} (\AA^3)	α_{zz} (\AA^3)	α (\AA^3)	TE
Adipodihydrazide	2	0.264	-0.118	0.0264	124.953	80.65	73.959	93.187	-606.300
4-Amino-3-hydrazino-5-mercaptop-1,2,4-triazole	1	0.197	-0.105	0.0279	119.937	70.384	36.893	75.738	-806.281
p- Aminobenzoyl hydrazide	1	0.185	-0.114	0.0350	155.363	95.23	35.325	95.306	-511.486
Benzenesulfohydrazide	1	0.220	-0.151	0.0518	130.509	95.836	57.001	94.449	-891.478
Benzoylhydrazine	1	0.210	-0.147	0.0513	122.17	90.797	33.915	82.294	-456.144
Biscyclohexanone oxalylidihydrazine	2	0.191	-0.145	0.0552	237.654	196.095	135.729	189.826	-915.868
Carbohydrazide	2	0.301	-0.101	0.0167	24.25	51.01	39.649	38.303	-335.781
1,2-Diformylhydrazine	1	0.224	-0.136	0.0411	63.452	42.689	15.469	40.537	-338.431
1,1-Diphenyl-2-picrylhydrazine	1	0.076	-0.180	0.2126	397.581	262.684	186.438	282.234	-1418.064
1,4-Diphenylsemicarbazide	1	0.200	-0.105	0.0273	222.926	134.266	98.99	152.061	-742.485
1,5- Diphenylcarbazide	2	0.195	-0.104	0.0277	181.264	168.833	108.494	152.864	-797.780
2-Hydrazinobenzothiazole	1	0.188	-0.120	0.0380	164.016	114.725	40.594	106.445	-833.221
2-Hydroxy-3-naphthoic acid hydrazide	1	0.143	-0.139	0.0675	226.405	143.927	44.264	138.199	-684.954
2-Hydroxyethylhydrazine	1	0.283	-0.074	0.0096	50.763	34.681	32.241	39.228	-265.602
Isonicotinic acid hydrazide	1	0.191	-0.161	0.0675	109.923	88.478	33.85	77.417	-472.159
Isophthaloyldihydrazide	2	0.197	-0.157	0.0629	165.777	120.121	49.827	111.908	-680.086
m-Nitrobenzhydrazide	1	0.158	-0.193	0.1175	146.725	113.637	37.779	99.380	-660.560
Malonyl dihydrazide	2	0.239	-0.131	0.0356	79.394	63.014	41.52	61.309	-488.390
Nicotinohydrazide	1	0.192	-0.154	0.0619	115.624	84.062	34.13	77.939	-472.159
4-Nitrophenylhydrazine	1	0.143	-0.154	0.0831	161.275	94.516	31.653	95.815	-547.256
o-nitrobenzhydrazide	1	0.145	-0.189	0.1231	132.965	112.279	50.003	98.416	-660.549
o-Nitrophenylhydrazine	1	0.129	-0.159	0.0977	124.133	119.901	31.698	91.911	-547.259
Oxalic dihydrazide	2	0.206	-0.151	0.0554	66.633	52.763	33.316	50.904	-449.067
p-Nitrobenzhydrazide	1	0.154	-0.196	0.1256	159.691	106.492	38.052	101.412	-660.560
Phenylazofornic acid-2-phenylhydrazide	1	0.102	-0.154	0.1167	295.842	125.279	107.978	176.366	-796.541
Phenylhydrazine	1	0.205	-0.084	0.0170	103.846	79.833	27.772	70.484	-342.829
Phenylhydrazine-4-sulfonic acid	1	0.159	-0.150	0.0710	169.605	103.413	58.595	110.538	-966.391
1-Phenylsemicarbazide	1	0.211	-0.096	0.0216	122.704	92.446	50.878	88.676	-511.488
Salicyl hydrazide	1	0.206	-0.130	0.0410	120.125	96.792	42.232	86.383	-531.325
Thiocarbohydrazide	2	0.205	-0.098	0.0233	73.677	58.524	30.051	54.084	-658.751
2-Thiophenecarboxylic hydrazide	1	0.193	-0.154	0.0619	114.836	88.793	34.051	79.227	-776.877
2,4,5-Trichlorobenzenesulfonyl hydrazide	1	0.130	-0.182	0.1269	216.121	148.077	88.305	150.834	-2269.910

metric tests. QSPR has become a useful technique to predict physicochemical properties that can be characterized based on information held within the molecular structure. In this

work, 18 such descriptors were used, which strongly depend on the molecule's geometry. The molecular descriptors used in the model were found to describe the thermal stability of the chemicals. From the correlation matrix, it was found that the highest positive charge, N-N bond distance and total energy are the descriptors that exhibit high correlation with onset temperature, and the oxygen balance, electrophilicity index and electron affinity are the descriptors showing high correlation for the heat of decomposition.

High-accuracy QSPR models were developed to predict onset temperature, T_o and heat of decomposition, $-\Delta H$ for a set of 32 noncyclic hydrazines. Reliability of the models was as-

Parameter	T_o	$-\Delta H$
R^2	0.895	0.978
R^2_{CV}	0.833	0.660
F	29.201	95.133
LOF	829.739	0.454

Table 3. Statistical parameters of QSPR models using GFA.

Chemical Name	$T_o(^{\circ}C)$		Log (Q)		Q(cal/g)	
	Experimental	Calculated	Experimental	Calculated	Experimental	Calculated
Adipodihydrazide	282.9	265.10	5.57	5.75	262.6	315.64
4-Amino-3-hydrazino-5-mercapto-1,2,4-triazole	228	200.60	5.33	5.20	207	180.57
p- Aminobenzoyl hydrazide	295	268.99	4.74	5.01	115	149.85
Benzenesulfohydrazide	147	146.83	5.96	5.95	387	385.05
Benzoylhydrazine	260	291.11	5.56	5.36	259	212.15
Biscyclohexanone oxalyldihydrazine	270	274.80	5.39	5.31	219	202.25
Carbohydrazide	238	237.61	6.20	6.10	491	444.90
1,2-Diformylhydrazine	234	230.09	5.72	5.72	304	304.98
1,1-Diphenyl-2-picrylhydrazine	170	175.57	6.83	6.84	926	934.47
1,4-Diphenylsemicarbazide	220	211.02	4.43	4.56	83.8	95.54
1,5- Diphenylcarbazide	204	225.91	5.28	5.23	196	186.78
2-Hydrazinobenzothiazole	237.6	251.08	5.19	5.13	180.3	168.24
2-Hydroxy-3-naphthoic acid hydrazide	209.6	241.08	4.35	4.21	77.8	67.16
2-Hydroxyethylhydrazine	251	246.18	5.48	5.48	240	240.07
Isonicotinic acid hydrazide	302.2	287.08	4.64	4.77	103.5	117.43
Isophthaloyldihydrazide	293	279.28	5.62	5.59	275	266.73
m-Nitrobenzhydrazide	222	225.80	6.34	6.26	567	521.48
Malonyl dihydrazide	208	209.46	6.34	6.36	564	576.57
Nicotinohydrazide	276.8	287.98	5.07	5.19	159.9	178.62
4-Nitrophenylhydrazine	178	180.21	6.07	6.07	432	432.69
o-nitrobenzhydrazide	277	296.82	6.67	6.61	789	739.03
o-Nitrophenylhydrazine	186	169.57	6.39	6.45	595	630.27
Oxalic dihydrazide	247.5	250.03	6.08	6.13	435.7	459.73
p-Nitrobenzhydrazide	225	219.91	6.17	6.24	478	513.13
Phenylazoformic acid-2-phenylhydrazide	162	159.90	5.75	5.75	314	313.64
Phenylhydrazine	295	270.82	4.97	5.02	144	151.06
Phenylhydrazine-4-sulfonic acid	291	286.13	4.31	4.33	74.8	76.01
1-Phenylsemicarbazide	217	221.59	5.32	5.18	204	177.24
Salicyl hydrazide	231	242.05	5.18	5.25	178	190.72
Thiocarbohydrazide	174	203.52	5.92	5.93	374.1	375.56
2-Thiophenecarboxylic hydrazide	316.7	295.11	4.97	4.89	144.1	133.28
2,4,5-Trichlorobenzenesulfonyl hydrazide	124	122.07	6.41	6.42	608	614.94

Table 4. Experimental and calculated calorimetric data for 32 noncyclic hydrazines.

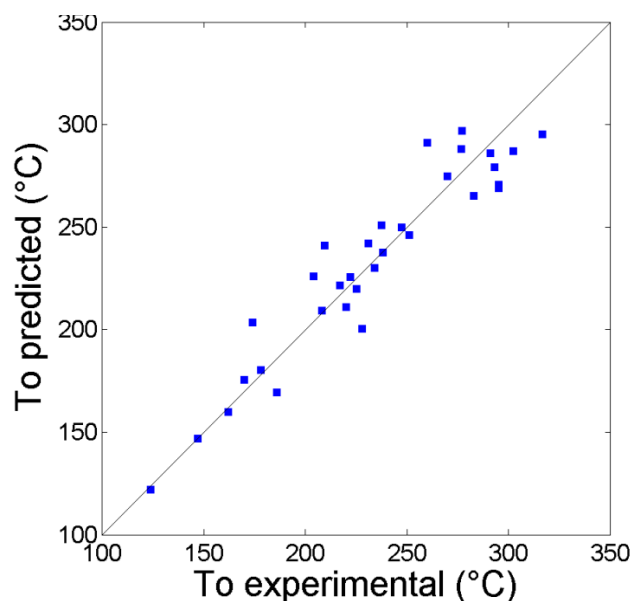


Figure 2. Calculated vs. experimental onset temperatures.

essed with statistical parameters (R^2 , R^2_{cv} and F value), which were favorable for each property (0.895, 0.833 and 29.201 for onset temperature, and 0.978, 0.660 and 95.133 for heat of decomposition).

For future work, the models can be expanded with a larger data set of noncyclic hydrazines, as well as to include validation using external test set. After collecting extensive experimental data, if it is found that parameters, such as concentration of the reactive material as well as other process conditions, have an influence on the estimation of the hazardous properties, then they should be included in future models as well. ☉

Acknowledgements

The financial support provided by the Mary Kay O'Connor Process Safety Center of the Department of Chemical Engineering at Texas A&M University for this research is gratefully acknowledged.

Nomenclature

- S_r Delocalizability index
- η Hardness/Chemical hardness (a.u.)
- μ Chemical Potential (a.u.)
- ω Electrophilicity index (a.u.)
- α Mean Polarizability (Å^3)

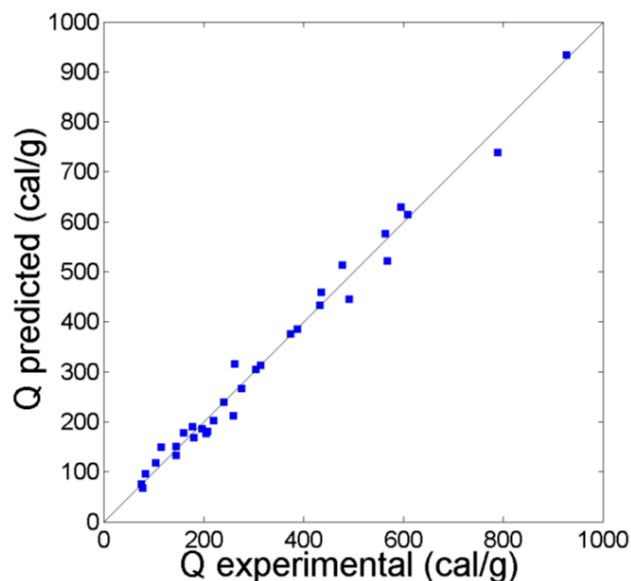


Figure 3. Calculated vs. experimental heat of decomposition.

Abbreviations

- QSPR Quantitative Structure Property Relationship
- GFA Genetic Function Approximation
- DSC Differential Scanning Calorimetry
- MARS Multivariate Adaptive Regression Splines
- EHOMO Eigen value of Highest Occupied Molecular Orbital
- ELUMO Eigen value of Lowest Unoccupied Molecular Orbital
- HPC Highest Positive Charge
- LNC Lowest Negative Charge
- NN Nitrogen-Nitrogen bond distance
- DM Dipole Moment
- OB Oxygen Balance
- MW Molecular Weight
- NHG Number of Hydrazine Groups
- TE Total Energy
- LOF Lack of Fit
- F-Value F-Value as it relates to the statistical F-Test

References

- Accelrys. (2006a). *Material studio user's manual*, version 5.0. San Diego, CA: Accelrys Inc.
- Accelrys. (2006b). *Materials studio release notes* (version 5.0). San Diego, CA: Accelrys Software Inc.
- Aldeeb, A.A., Rogers, W.J. & Mannan, M.S. (2002). Theoretical and experimental methods for the evaluation of reactive chemical hazards. *Process Safety and Environmental Protection*, 80(3), 141-149.
- Ando, T., Fujimoto, Y. & Morisaki, S. (1991). Analysis of differential scanning calorimetric data for reactive chemicals. *Journal of Hazardous Materials*, 28(3), 251-280.
- CCPS. (1995). *Guidelines for chemical reactivity evaluation and application*

	T_o	$-\Delta H$
Average absolute deviation	12.156 K	18.456 cal/g
Average absolute relative deviation (%)	5.112	7.465
Average percent bias (%)	-0.399	-0.492

Table 5. Statistical evaluation for the data set using GFA.

to process design. New York, NY: Center for Chemical Process Safety of the American Institute of Chemical Engineers

Fayet, G., Rotureau, P., Joubert, L. & Adamo, C. (2009). On the prediction of thermal stability of nitroaromatic compounds using quantum chemical calculations. *Journal of Hazardous Materials*, 171(1-3), 845-850.

Frisch, M.J., Trucks, G.W., Schlegel, H.B., Scuseria, G.E., Robb, M.A., Cheeseman, R., et al. (2003). Gaussian 03. Wallingford, CT: Gaussian Inc.

Gharagheizi, F. (2009). A QSPR model for estimation of lower flammability limit temperature of pure compounds based on molecular structure. *Journal of Hazardous Materials*, 169(1-3), 217-220.

Grewer, T. (1991). The influence of chemical structure on exothermic decomposition. *Thermochimica Acta*, 187, 133-149.

CHEMINDUSTRY.ru. Hydrazine: Chemical product information. Retrieved from <http://chemindustry.ru/Hydrazine.php>.

Karelson, M., Lobanov, V.S. & Katritzky, A.R. (1996). Quantum-chemical descriptors in QSAR/QSPR studies. *Chemical Reviews*, 96(3), 1027-1044.

Katritzky, A.R., Rachwal, P., Law, K.W., Karelson, M., Lobanov, V.S. (1996). Prediction of polymer glass transition temperatures using a general quantitative structure-property relationship treatment. *Journal of Chemical Information and Computer Sciences*, 36, 879-884.

Lu, Y., Ng, D. & Mannan, M.S. (2011). Prediction of the reactivity hazards for organic peroxides using QSPR approach. *Industrial & Engineering Chemistry Research*, 50(3), 1515-1522.

Miyake, A., Kimura, A., Ogawa, T., Satoh, Y. & Inano, M. (2005). Thermal hazard analysis of hydrazine and nitric acid mixtures. *Journal of Thermal Analysis and Calorimetry*, 80(2), 515-518.

NCBI PubChem. Retrieved January 2010 from <http://pubchem.ncbi.nlm.nih.gov>.

Pan, Y., Jiang, J., Wang, R., Cao, H. & Cui, Y. (2009). Predicting the autoignition temperatures of organic compounds from molecular

structure using support vector machine. *Journal of Hazardous Materials*, 164(2-3), 1242-1249.

Parr, R.G. & Pearson, R.G. (1983). Absolute hardness: Companion parameter to absolute electronegativity. *Journal of the American Chemical Society*, 105(26), 7512-7516.

Parr, R.G., Szentpaly, L.V. & Liu, S. (1999). Electrophilicity index. *Journal of the American Chemical Society*, 121(9), 1922-1924.

Patel, S.J., Ng, D. & Mannan, M.S. (2009). QSPR flash point prediction of solvents using topological indices for application in computer aided molecular design. *Industrial & Engineering Chemistry Research*, 48(15), 7378-7387.

Rogers, D. & Hopfinger, A.J. (1994). Application of genetic function approximation to quantitative structure-activity relationships and quantitative structure-property relationships. *Journal of Chemical Information and Computer Sciences*, 34(4), 854-866.

Saraf, S.R., Rogers, W.J. & Mannan, M.S. (2003a). Application of transition state theory for thermal stability prediction. *Industrial & Engineering Chemistry Research*, 42(7), 1341-1346.

Saraf, S.R., Rogers, W.J. & Mannan, M.S. (2003b). Prediction of reactive hazards based on molecular structure. *Journal of Hazardous Materials*, 98(1-3), 15-29.

Saraf, S.R., Rogers, W.J. & Mannan, M.S. (2003c). Using screening test data to recognize reactive chemical hazards. *Journal of Hazardous Materials*, 104(1-3), 255-267.

Schirmann, J.Q. & Bourdauducq, P. (2002). Hydrazine: Ullmann's encyclopedia of industrial chemistry, Weinheim: Wiley-VCH.

Shanley, E.S. & Melhem, G.A. (1995). The oxygen balance criterion for thermal hazards assessment. *Process Safety Progress*, 14(1), 29-31.

Shi, L.M., Fan, Y., Myers, T.G., O'Connor, P.M., Paull, K.D., Friend, S.H., et al. (1998). Mining the NCI anticancer drug discovery databases: Genetic function approximation for the QSAR study of anticancer ellipticine analogues. *Journal of Chemical Information and Computer Sciences*, 38(2), 189-199.

Incident Analysis of Major Crowd Stampedes

Jacques Albert, Qingsheng Wang, Tingguang Ma and Michael Larranaga

Abstract

In this work, the fundamental theories explaining the features relevant to crowd, rumor and panic were re-viewed. Following this information, a list of major crowd stampede incidents was compiled. Several factors affecting crowd stampedes were identified and analyzed based on the principles of crowd movement, rumor and panic. This incident analysis included a system of categorizing the types of crowd stampede initiations. It was found that the most significant variable in intense stampede initiations is the social environment in which the crowd exists. The study also indicated that rumor and panic go hand-in-hand in uncertain and ambiguous situations. This work could provide insights into emergency response management of future crowd stampede incidents.

Keywords

Crowd stampedes, emergency response, rumor and panic, incident analysis

Introduction

Rumor, panic and crowds have been studied over the past century. However, in most of these studies, they are addressed individually. Cantril (1943) and Quarantelli (1954) have studied panic, as well as Mawson (2005) in more recent years. Crowd dynamics have been studied and modeled in all different manners in relation to normal flow and emergency situations. Likewise, rumor has been studied from the psychological and sociological perspectives in the context of collective behavior. While each of these theories has its own unique point of view, intent and focus, they are usually divided into two major areas: crowds and rumors.

The research in crowds has generally fallen into two categories. The first type of research looks at how crowds function under normal circumstances in various environments and consistencies. Observations of collective and individual behavior are used to generate predictions or models of the general flow of pedestrian traffic. Often this is with the intent of facilitating safe and efficient flow patterns and involves multiple and intersecting flows. The other research studied is that of pedestrian flow in emergency situations. This study is typified by high-stress situations in which the entire crowd has a single urgent goal, for example, getting away from a dangerous point

in space or getting to a desirable point, be it an escape location or another object of desire.

The topic of panic has been studied extensively, and the way it is defined and described has varied over the years. Cantril (1943) first addressed the topic of panic. In his paper, he differentiated between two kinds of panic. The first is a crowd phenomenon caused by an immediately apparent danger. Examples he gives include “fires in theaters, sinking ships, etc.” (Cantril, 1943). The type of panic Cantril focused on is the kind of panic that appears to the casual observer to be completely irrational. These panics seemed to be driven not by outside forces, but by psychological forces.

In characterizing these panics, Cantril proposed several factors that may contribute. Anxiety due to news of impending danger or past social experience may influence an individual or a group to be susceptible to news that seems to verify that sense of anxiety. Whether the threat is legitimate or imagined, this confirmation of anxiety can lead to a panic by creating a situation in which ignorance is not detected and the situation is handled with the existing information. Lacking correct information, but not knowing that their information is false, people’s ability to deal with that situation may be impaired so much as to make them feel trapped. This is a recipe for panic. This ignorance is itself a cause of panic according to Cantril. Even if people are in a state of mind to seek information and to behave rationally, they may not have the tools to do so. Given a threatening situation, people who do not have an explanation may lack standards against which to judge the situation, may judge against the wrong standards in the wrong contexts or may go to others who have already accepted the wrong explanation as an authority.

Quarantelli (1954) built upon this simple examination with his paper, “The Nature and Conditions of Panic.” He attempted to clarify the definition of panic and its features and the condi-

Jacques Albert is a student of Fire Protection and Safety at Oklahoma State University (OSU).

Qingsheng Wang, Ph.D., is assistant professor of fire protection and safety and assistant professor of chemical engineering (graduate faculty) at OSU. He can be contacted at qingsheng.wang@okstate.edu.

Tingguang Ma, Ph.D., is assistant professor of fire protection and safety at OSU.

Michael Larranaga, Ph.D., P.E., CSP, CIH, is Simplex professor and department head of fire protection and safety at OSU.

tions that cause it. The first feature of panic he addresses is the most apparent. Panic is typified by flight, and more specifically this flight is away from danger. He pointed out that while to an outside observer this flight may appear to be irrational and unfocused, it is likely perfectly rational to the fleeing person based on the information at his or her disposal. He argued that these decisions may be made based on both the habits of the individual and interaction with others dealing with the same situation. Quarantelli also clarified that panic is not antisocial behavior, but is rather nonsocial behavior.

In recent years, specific research into the nature of panic has been done by Mawson (2005). One of his primary caveats is the definition of the phenomenon, which he discusses as being individual and collective flight behavior of varying intensity. Mawson addressed a theory that was built upon the original panic framework in regards to flight from indeterminate dangers. He cites the idea that those who flee upon seeing others fleeing are doing so because “to see someone running wildly is prima facie evidence that he is seeking to escape through limited exits . . . and that he is anxious. Furthermore, this observed flight is a precipitating event for the observer, and gives rise to the belief that something frightening is present, even though this ‘something’ may not be identical to that which caused the original flight” (Smelser, 1963).

In contrast, Mawson proposed that in situations where there are social group ties between the observer and those fleeing, the observer’s flight may be interpreted “not as an attempt to escape real or imagined dangers but as an attempt to maintain proximity with those who started the run, including the group leader, that is, an affiliative response designed to reaffirm social bonds” (Mawson, 2005). It stands to reason that even lesser social ties than those of men in combat may elicit similar, if less acute, affiliative responses. He proposed that flight is actually part of a duality of response to a dangerous situation consisting of both flight from danger and flight toward people and places viewed as familiar.

The implications of this theory relate to the context of the individuals in the dangerous situations with respect to familiar people and places. If individuals are near attachment figures, intense affiliative behavior is the most likely response, followed by group flight. However, if an individual is not near any attachment figures, flight and affiliation become much more likely. This newer theory fits nicely with the common observance in egress studies that people in emergency evacuations in unfamiliar places tend to leave the way they came in. These people are fleeing from the danger, and toward the most familiar place, in this case the only exit or entrance that they have been to before (Mawson, 2005).

As summarized by Helbing, older methods of studying crowd movement relied on mathematical models, such as queuing models, transition matrix models and stochastic models (Helbing, et al., 2002). These were primarily concerned with orderly pedestrian behavior in normal circumstances and failed to take into account self-organization effects that result from individuals in the crowd exhibiting intelligent decision-making. Therefore, more recent efforts have focused on direct simulation of individual pedestrian motion, or microsimulation

of pedestrian crowds, to include behavioral force models, cellular automata and AI-based models (Helbing, et al., 2002).

With regards to normal pedestrian behavior, Helbing observes that pedestrians exhibit several tendencies. One is that they exhibit a “strong aversion to taking detours or moving opposite to the desired walking direction, even if the direct way is crowded,” but “normally choose the fastest route... not the shortest one” (Helbing, et al., 2002). They prefer to walk with an individual desired speed, which varies based on demographic and environment. They like to keep a certain distance from others and from obstacles; this distance becomes smaller in higher densities or at higher speeds, but pedestrians may form groups that behave similar to single pedestrians. Helbing’s generalized force model exhibits some characteristic crowd phenomena that are of interest, which he explains in his report. Helbing’s pedestrians tend to form lanes of travel that allow for opposing pedestrian flow direction to travel smoothly past each other under normal circumstances. Likewise, at bottleneck openings, pedestrians going through in one direction relieve pressure from their side of origin as they and pedestrians behind them travel through the opening. At a certain point, this pressure difference between the two sides is sufficient that the higher pressure of the opposing flow will dominate the opening, and the process will repeat in the other direction.

However, in panic situations, a phenomenon called “freezing by heating” occurs, whereby the increased urgency of two opposing pedestrian flows leads to breakdown of organizational phenomena, and instead the two opposed flows deadlock into a solid formation where neither side can pass. Similarly, increased speed and urgency at openings even going in one direction can lead to clogging and the formation of arches of pedestrians, which result in periodic passing of bunches of pedestrians when an arch collapses. Helbing also observed that at extremely high crowd densities and low flow rates, turbulent flows become apparent in the crowd, resulting in stop-and-go waves, shock waves that propagate through the mass of pedestrians with enough force to knock people off their feet (Helbing, et al., 2007).

One aspect of crowds that appears to have been understudied is methods of communication within crowds. Almost all of the crowds modeling simulations that currently exist assume that every individual in the crowd is aware of all of the relevant information, such as the existence of the danger, the location of the danger, the geometry of the environment and the location of the exits. Alternatively, some methods crudely simulate the ability of pedestrians to “discover” very basic information about the environment, such as the location of exits, or at the very least act on this information without truly remembering or storing it (Bandini, et al., 2007). While some simulations allowed for a very basic communication between adjacent individuals, this communication was extremely limited in scope (as mentioned, to the location of exits) and method (physical contact) as exemplified by Henein and White (2010).

The most comprehensive model found was a computer model combining high-density autonomous crowds for local motion simulation with a system called Multi-Agent Communication for Evacuation Simulation (MACES) for communica-

tion and roles, both systems using psychological information (Gomez, 2006). Even this simulation, however, does not fully address advanced communication behaviors that might be exhibited, such as coordination in prepanic scenarios, or nonsimultaneous emergency awareness and evacuation initiation.

The study by McHugh, et al. (2010) found that when all participants in a crowd are displaying the same emotion, humans are highly accurate at identifying that emotion, and the more people in a crowd displaying an emotion, the faster and more accurately they can be perceived. This study also found no significant correlation between the size of a crowd and the time required or accuracy in identifying the emotion.

With the review of fundamentals of crowds, rumor, panics and crowd movement modeling, in this work, we focus on collecting major crowd stampede events. In an effort to combine this framework of theories regarding rumor, crowd and panic, an attempt must be made to fit it onto actual events. An overview of cases and a brief examination of relevant incidents can provide an indication of the applicability of these frameworks to future study and can suggest directions in which to further explore their relationship with more exhaustive means. Based on actual incident analysis, factors that affect crowd stampede were identified and the stampede initiations were classified. This work can provide insight of effective crowd management

in emergency response.

Methods

The review of incidents was focused on major crowd stampede events for which reliable sources of information could be found. Events from all over the world were included. A conscious effort was made to exclude events in which crowd stampedes or other crowd-related factors appeared to be incidental or relatively unimportant. The overall list was allowed to include a few incidents in which crowd stampedes played a major part but were not the primary cause of death and injury, as a means of comparison to primarily crowd-centric incidents. The information recorded and analyzed is that information, which was deemed to be helpful in classifying the rumor-panic relationship in regards to the crowd stampede event.

A list of incidents was compiled from various other lists of crowd disasters available on the Internet. Individual incidents that were located independent of these lists were also included and evaluated. From this list, one or more sources were found for each incident. If no source could be found for an incident, it was removed from the list. From the information in these sources, each incident was evaluated to determine whether it fell within the scope of the review. If it did not, that event was eliminated from the list. If a source was available but the information

ID	Year	Location	Physical Env.	Fat.	Inj.	Instigator	Rumor	Social Env.	Danger Obv.	Fear-Based Inst.
1	1883	Brooklyn	Bridge	13	26	Fall & Scream	Collapse	New Type of Bridge	No	Yes
2	1883	Sunderland	Hall	183	100	Offer of Gifts	None	Children	No	Yes
3	1896	Khodynka	Field	1,429	644	Rumor	Insufficient Gifts	Hungry People	No	Yes
4	1902	United States	Temple	115	78	Scream	Fire		No	Yes
5	1903	United States	Theater	602	250	Fire	None		Yes	Yes
6	1908	South Yorkshire	Hall	16	40	Offer of Seats	None	Children	No	No
7	1913	United States	Theater	73		Fire	None	Children	No	Yes
8	1928	United States	Hall	40		Fire	None		Yes	Yes
9	1940	United States	Club	198		Fire	None		Yes	Yes
10	1942	United States	Club	492		Fire	None		Yes	Yes
11	1943	United Kingdom	Shelter	173		Fall/Loud Noise	None	Frequent Bombings	No	Yes
12	1954	India	Field	350	2,000	Arrival of Holy Men	None		No	No
13	1955	Chile	Stadium	6			None	Sports	No	No
14	1956	Yahiko	Temple	124		Offer of Gifts	None		No	No
15	1964	Peru	Stadium	318	500	Referee Call	None	Sports	No	No
16	1968	Argentina	Stadium	74	150	Locked Gate	None	Sports	No	No
17	1971	United Kingdom	Stadium	66	145	Rail Failure	None	Sports	No	No
18	1971	Brazil	Stadium	4	1,500	Fight		Sports	No	No
19	1973	United States	Club	32		Fire	None		Yes	Yes
20	1974	United States	Club	24		Fire	None		Yes	Yes
21	1974	Egypt	Stadium	49	50		None	Sports	No	No
22	1976	United States	Club	25		Fire	None		Yes	Yes
23	1976	Cameroon	Stadium	2		Fight	None	Sports	No	No
24	1976	Haiti	Stadium	6		Firecracker	None	Sports	No	Yes
25	1977	United States	Club	165		Fire	None		Yes	Yes
26	1979	United States	Stadium	11	24	Doors Opening	None		No	No
27	1982	U.S.S.R.	Stadium	340		Sudden Cheering	None	Sports	No	No
28	1985	Brussels	Stadium	39		Wall Collapse	None	Sports	No	No

Table 1. Incident review of crowd stampedes—Part 1.

ID	Year	Location	Physical Env.	Fat.	Inj.	Instigator	Rumor	Social Env.	Danger Obv.	Fear-Based Inst.
29	1988	Nepal	Stadium	93		Hail	None	Sports	Yes	Yes
30	1989	United Kingdom	Stadium	95		Gate Opening	None	Sports	No	No
31	1990	Saudi Arabia	Tunnel	1426			None		No	No
32	1990	United States	Club	87		Fire	None		Yes	Yes
33	1990	Spain	Club	43		Fire	None		Yes	Yes
34	1991	Orkney	Stadium	42		Fight	None	Sports	No	Yes
35	1991	Chalma	Temple	40	35		None		No	No
36	1991	South Africa	Stadium	42	50	Fight	None	Sports	No	Yes
37	1993	Hong Kong	Street	20	71		None		No	No
38	1993	United States	Stadium	0	69		None	Sports	No	No
39	1994	Mecca	Bridge	250			None		No	No
40	1994	Nagpur	Field	114		Minister Arrival/Police Attack	None		Yes	Yes
41	1996	Guatemala City	Stadium	84	150	Door Opening	None	Sports	No	No
42	1998	Mecca	Bridge	119			None		No	No
43	1999	Minsk	Metro Station	54		Thunderstorm	None		Yes	Yes
44	2000	Denmark	Field	18	80		None		No	No
45	2000	Zimbabwe	Stadium	12		Tear Gas	None	Sports	Yes	Yes
46	2001	Bulgaria	Club	7	24		None		No	No
47	2001	Saudi Arabia	Bridge	35			None		No	No
48	2001	Ghana	Stadium	126	150	Tear Gas	None	Sports	Yes	Yes
49	2001	Cote d'Ivoire	Stadium	1	39	Tear Gas	None	Sports	Yes	Yes
50	2001	Congo	Stadium	14	12	Tear Gas	None	Sports	Yes	Yes
51	2001	South Africa	Stadium	43	250	Goal	None	Sports	No	No
52	2003	United States	Club	21		Pepper Spray	Terrorist Attack	Terrorist Attacks	Yes	Yes
53	2003	United States	Club	97		Fire	None		Yes	Yes
54	2003	Saudi Arabia	Bridge	14			None		No	No
55	2003	Pakistan, Islamic	Temple	7	20	Fire	None		Yes	Yes
56	2003	Sudan	Street	31	48	Offer of Gifts	None		No	No
57	2004	China	Bridge	37	15	Fall	None		No	No
58	2004	Mecca	Bridge	244	244		None		No	No

Table 1. Incident review of crowd stampedes—Part 2.

from that source was insufficient to classify the event properly, that event was removed from the list. This mostly consisted of removing incidents for which no fatality data could be found. From this process, a list was created consisting of 97 individual crowd disasters of varying types from all over the world. It should be noted that all of these crowd disasters are not related with the oil and gas industry or chemical industry. A separate study that focuses on the emergency response management of crowd panic in chemical industry will be conducted later.

The two primary sources of the initial lists from which the majority of events were identified were the Wikipedia article on human stampedes and the Disaster Database run by Walter G. Green III, University of Richmond. For the incidents found in the list retrieved from Wikipedia, an independent news source was located to pull the actual information. If necessary, multiple sources were used to piece together the necessary information. For incidents that were found in the Disaster Database, the database itself is cited as the source of information. Each entry in the database includes the citation for all information in the entry. If additional information could be located via other sources, this information was included in the table.

Results & Discussion

Using the sources discovered while paring the list, each event was examined, several points of data were recorded into a table and the circumstances of the event were interpreted into several factors to facilitate classification. The incidents are shown in Table 1, which is listed by date from oldest to the most recent.

Factor Selection

The factors chosen to be listed in the table are as follows:

- ID—This is a table-specific identification number, which was provided to differentiate between similar events, especially those that occurred in the same place and in the same year.
- Year—The date information was limited to the year. This is mainly useful for differentiating between events that occurred in the same place and to facilitate any possible trends in events that might be gleaned from similar categories.
- Location—The location is the country in which the event took place. This was included to differentiate between events and to facilitate possible trends within a location.
- Physical Environment—This factor is an attempt to classify events based on the specific physical characteristics in which the event occurred.

ID	Year	Location	Physical Env.	Fat.	Inj.	Instigator	Rumor	Social Env.	Danger Obv.	Fear-Based Inst.
59	2004	Saudi Arabia	Shop	3		Offer of Gifts	None		No	No
60	2004	Togolese	Stadium	4	8	Sudden Darkness	None	Sports	No	No
61	2004	Togolese	Field	13	50		None		No	No
62	2005	India	School	42	37	Offer of Gifts	None		No	No
63	2005	India	Temple	256			None		No	No
64	2005	Bangladesh	Field	6	12		None		No	No
65	2005	Iraq	Bridge	500		Rumor	Suicide Bomber	Frequent Attacks	No	Yes
66	2005	Madagascar	Stadium	2	25		None	Sports	No	No
67	2005	India	Street	16	18	Rumor	Dam Burst	Torrential Rain	No	Yes
68	2005	Saudi Arabia	Airplane	1	62	Bomb Threat	None		No	Yes
69	2006	Mecca	Bridge	345	1,000		None		No	No
70	2006	Yemen	Stadium	51	230	Fall	None		No	No
71	2006	Philippines	Stadium	66		Scream of Bomb	Bomb		No	Yes
72	2006	Korea	Stadium	34			None		No	No
73	2006	Pakistan, Islamic	Stadium	29	70	Fall	None		No	No
74	2007	India	Metro Station	13	30		None		No	No
75	2007	China	Shop	3	31	Fall	None		No	No
76	2007	Zambia	Stadium	12	50		None		No	No
77	2007	India	Bridge	11	20	Fall	None		No	No
78	2008	Mexico City	Club	12		Police	Arresting		Yes	Yes
79	2008	India	Bridge	162	47	Rumor	Landslide		No	Yes
80	2008	Congo	Stadium	11		Tear Gas	None		Yes	Yes
81	2008	India	Temple	168	425	Rumor	Bomb		No	Yes
82	2008	United States	Shop	1	4	Sale	None		No	No
83	2009	Ivory Coast	Stadium	22	132		None		No	No
84	2009	Pakistan, Islamic	Street	20	15	Baton Push	None		No	Yes
85	2010	India	Temple	63	44	Offer of Gifts	None		No	No
86	2010	Amsterdam	Field	0	24	Scream	None		No	Yes
87	2010	Germany	Tunnel	18	200		None		No	No
88	2010	Cambodia	Bridge	347	755	Fall	None		No	No
89	2010	India	Temple	102	44	Vehicle Accident	None		No	No
90	2010	Mali	Temple	26	55	Death	None		No	No
91	2010	Uganda	Field	1	140		None		No	No
92	2010	India	Field	5	2	Rain	None		No	No
93	2010	South Africa	Stadium	0	16		None		No	No
94	2010	Jordan	Stadium	0	250	Fan Attack	None		Yes	Yes
95	2010	India	Metro Station	2	15		None		No	No
96	2011	India	Temple	102		Vehicle Accident	None		Yes	Yes
97	2011	Mali	Temple	36	112	Scream	None		No	Yes

Table 1. Incident review of crowd stampedes—Part 3.

•Fatalities—This statistic is included as a way to relate the relative severity of the various incidents to each other.

•Injuries—Much like fatalities, this is included where available to help define the relative severity of incidents.

•Instigating Event—The instigating event is listed when a discrete, identifiable event or suddenly apparent condition is readily and specifically identified in the source material.

•Rumor—If there was a documented possibility or mention of a rumor that directly contributed to the occurrence of the event, the rumor topic is listed here.

•Social Environment—Barring an extensive survey of the culture and recent history of every society and subgroup involved in the incident, the social environment information cannot be sufficiently filled out. However, when that societal

factor was readily apparent and documented in the source material, it was included here.

The following two questions were also included to facilitate the primary method of categorization to be used:

1) Danger obvious? This question refers to whether or not there was a documented, reasonable indication that there was an actual, verifiable and immediate danger readily apparent to those individuals who were involved in the onset of the incident.

2) Fear-based instigation? Likewise, this question refers to whether or not the instigating event as interpreted by those involved in the onset of the event could reasonably have been seen as eliciting a fear response prior to the actual onset of the event.

The selection of the factors to include was based on the idea that the three factors that can possibly contribute to a behavior

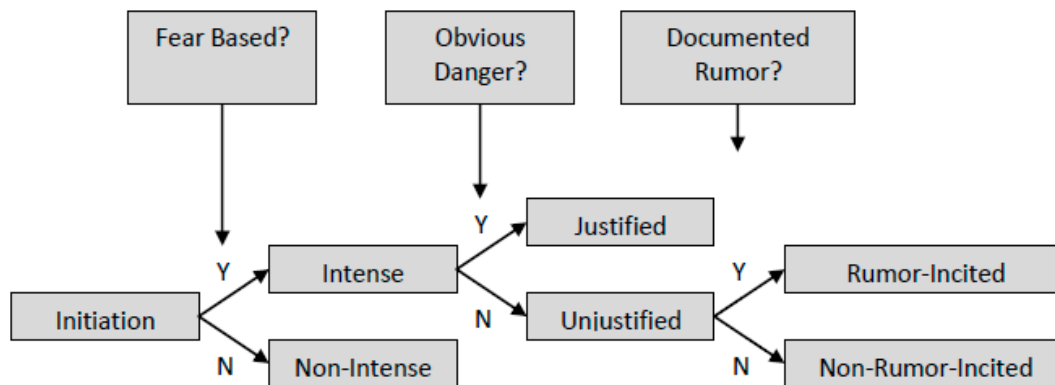


Figure 1. Decision tree.

are the individual, the physical environment and the social environment in which that individual exists. This refers to the idea that an individual has a certain set of behavioral tendencies and knowledge; s/he must function within the physical environment to include the people around him or her and the geometry of the space s/he is in and the social environment, including culture, group norms and recent history in which s/he operates.

The physical environment was recorded by the simplest descriptor possible to differentiate between categories of environments, with a mind toward keeping the descriptors relatable. Too specific a descriptor would be largely unhelpful as each event would appear to take place within its own unique location, with several factors all contributing to the incident. While this is certainly a valid area of interest, the scope of the analysis does not require this level of detail.

This is particularly evident due to the general similarity between the environment types, which typified the crowd events, and the fact that the most prominent physical factor in most of the events as it related to the rumor-panic relationship was the people, rather than the geometry of the environment. The social environment was the most difficult area to find information. Further case-by-case study might reveal more information, which could clarify this, the seemingly most important factor in the rumor-panic relationship to the crowd stampede.

Factor Analysis Crowd Movement

Crowd movement as it applies to this study is of concern only in the panic context. Normal crowd movement is not a significant contributing factor to the development of a stampede.

Initiation Types	# of Initiations	# of Fatalities
Non-Intense	54	5,269
Intense	42	5,417
Justified	24	2,372
Unjustified	18	3,045
Non-Rumor-Incited	13	770
Rumor-Incited	5	2,275
Total	96	10,686

Table 2. Summary of crowd stampede initiation data.

pede. Stampede crowd movement is typified by the movement of a large mass of people without regard for the consequences of that movement. This might be as a result of panic or it might be as a result of ignorance. A panicking crowd might push forward away from a perceived danger, or toward an object of desire, with such intensity that collectively the consequences of that pushing cease to matter. Or, a crowd section may be aware

of the consequences of their movement (trampling or crushing others) but may be forced to continue by the mass of people behind them who are not aware of these consequences.

Crowd movement problems like this arise when the density of the crowd is too great. This can occur in relatively open areas with massive amounts of people or in smaller confined spaces like halls and doorways, even with smaller amounts of people. The physical environment is the most apparent contributing factor to this aspect. All of the incidents studied took place under essentially identical circumstances with regards to this factor: too many people, too close together. No significant analysis can be made from the information used.

Panic

The relevant factors of panics in this study are the tendency for panic to occur where there is a perception of helplessness, impending danger and limited or rapidly closing escape routes. By the very nature of the studied events, these panics take place in densely packed crowds in which the mass of people and the small space are enough to give the sense of limited escape routes. The impending danger that occurs in the cases that will be classified as panics might be real or imagined, but they are mostly of the type in which individuals within the crowd have little to no hope of directly dealing with the danger.

The usual definitions of panic refer to an ongoing state of an individual or group's thought process. However, for the purposes of this study, this type of panic is largely irrelevant. This study does not take into account the influence of an active panic situation. Rather, the focus here is on the instant of initiation of a stampede. It is presumed that such an initiation happens within a spectrum of agitation at either an individual or group level. Therefore, for the purposes of this study, panic can be defined as an intense, fear-based stampede of people within a crowd. No statement or judgment is made about the rationality of this action, except as it applies to rumor. Therefore, rather than apply the label of "panic" along with the associated connotations of arguable rationality and ongoing state of mind, the term "intense" is used to identify this behavior.

Rumor

One significant finding of this study is that factors that precipitate and facilitate rumor invention and propagation are essentially the same factors, which precipitate and facilitate panic. Motivations for participation in rumor-spreading coincide with motivations for panic and exist as a stage in the panic process. It might be expected that such an activity could help mitigate the possibility of panic. The coincidence of rumor and panic creates the possibility of panic, which will result in rumor creation and transmission. For the purposes of this study, therefore, the concept of rumor is defined as unverified information, which is communicated through unofficial means throughout a crowd.

Categories of Stampede Initiation

Using these factors, a classification system for stampede initiation becomes clear at the intersection of these separate subjects. This classification is based on the characteristics of the origin of the motivation of the individuals in the crowd. The decision tree that led to these categories is summarized in Figure 1. A quantitative summary of these categories is presented in Table 2.

Non-Intense

Fifty-four incidents of this type were recorded, making this by far the most common type of crowd stampede observed in this analysis. These initiations are characterized by a lack of an apparent danger obvious to all those involved in the initiation before the event occurs and an initiating event that likely would not reasonably incite fear in a large portion of those involved in the initiation. Sometimes the instigating event is in fact obvious to all those involved in the initiation of the stampede, but it is not a danger. When the initiating event was documented for these types of stampedes, they tended to be accidental, low-impact or related to a positive desire. Typical instigators are someone slipping or tripping and setting off a chain reaction or the sudden actual or apparent possibility of access to an object of desire, be it a location (access to an event) or a thing (free food, gifts, etc.). Arguable entries in this category include the repeated appearance of sudden rainstorms of varying intensity triggering a desire to get out of the rain. These are negative motivators but are not truly fear-based.

Intense Unjustified

Eighteen incidents of this type appear in the list. Intense unjustified stampede initiations are those events in which there is a significant danger perceived by all of those involved in the initiation, and the stampede is motivated by specific fear of that danger. This danger might be perceived directly by the participants, leaving no time for rumor propagation, or information about the perceived danger may reach the participants by way of some sort of rumor. However, the perceived danger of these stampedes is not an actual ongoing threat to a significant portion of those involved. Typical initiating events for these types of stampedes are loud sudden noises or screams and false shouts identifying a danger.

Intense Rumor-Incited

Five incidents of this type appear in the list. This type of stampede is a subset of the intense unjustified category. In this category, there is an intense fear and panic reaction to a danger, which not only does not actually exist, but to which there has been no direct observation of evidence to support the existence. This type of stampede is, as far as can be documented, as close to a spontaneous and unprovoked eruption of panic as was found in this list. Three of the five incidents in this category had a readily apparent and documented social environmental contributing factor.

Intense Justified

Twenty-four incidents in the list can be classified as intense justified stampede initiation. These are incidents in which there is an observable significant threat evident to all of the people involved with the initiation of the stampede. This type of stampede is the most straightforward of the categories and is typified by two very common instigators. The first is fire, and the second is some sort of outside group attacking the crowd. Most of the events fall into one of these two categories, and most of the outside groups identified in this list are police officers either pushing, hitting or otherwise physically advancing on the crowd or firing tear gas into the crowd.

Conclusions

An effort should be made to fully understand how a crowd panic might be instigated and how the people in the stampede might behave in emergency response management of major stampedes. Those efforts might give further insight into how spontaneous stampedes happen and how the extremely common phenomenon of distant masses of the crowd unknowingly contributing to mass casualties further ahead can be mitigated or avoided.

The study found that the most significant variable in intense stampede initiations is the social environment in which the crowd exists. It was also discovered that rumor and panic go hand-in-hand in uncertain and ambiguous situations. Understanding the anxieties and cultural values of the crowd might go toward being prepared to mitigate panic and rumor-spreading in emergency. If it is known what the likely fear environment of the crowd are and what the most probable triggers for those fears could be, then it becomes easier to determine the most effective action to reduce the likelihood of this occurring. This work could also provide effective information or lessons for emergency response management in other industries in case of incidents. ☺

References

- Bandini, S., Federici, M.L. & Vizzari, G. (2007). Situated cellular agents approach to crowd modeling and simulation. *Cybernetics and Systems*, 38(1), 729-753.
- Cantril, H. (1943). Causes and control of riot and panic. *The Public Opinion Quarterly*, 7(4), 669-679.
- Gomez, N.P. (2006). Modeling realistic high-density autonomous agent crowd movement: Social forces, communication, roles and

psychological influences. Dissertations, University of Pennsylvania, Philadelphia, PA.

Helbing, D., Farkas, I.J., Molnar, P. & Vicsek, T. (2002). Simulation of pedestrian crowds in normal evacuation situations. In M. Schreckenberg & S.D. Sharma (Eds.), *Pedestrian and evaluation dynamics* [pp. 21-58]. Berlin: Springer

Helbing, D., Johansson, A. & Al-Abideen, H.Z. (2007). The dynamics of crowd disasters: An empirical study. *Physical Review E*, 75, 046109.

Henein, C.M. & White, T. (2010). Microscopic information processing and communication in crowd dynamics. *Physica A*, 389, 4636-4653.

Mawson, A.R. (2005). Understanding mass panic and other collective responses to threat and disaster. *Psychiatry*, 68(2), 95-113.

McHugh, J.E., McDonnell, R., O'Sullivan, C. & Newell, F.N. (2010). Perceiving emotion in crowds: The role of dynamic body postures on the perception of emotion in crowded scenes. *Experimental Brain Research*, 204(3), 361-372.

Quarantelli, E.L. (1954). The nature and conditions of panic. *The American Journal of Sociology*, 60(3), 267-275.

Smelser, N.J. (1963). *Theory of collective behavior*. New York, NY: Free Press of Glencoe.

Extracting Kinetic Information Using Power Measurements From Isothermal Calorimeters

Subramanya Nayak, M. Sam Mannan and Simon Waldram

Abstract

In this study, we demonstrate that both the heat of reaction and kinetic constants of a single chemical reaction can be estimated from a temporal power measurement derived from an isothermal reaction calorimeter. Appropriate mathematical models are developed to extract kinetic information. Both the batch and semi-batch mode of operation are considered. The derived equations are applied to the hydrolysis reaction of acetic anhydride so as to estimate enthalpy of reaction, kinetic constants and activation energy. The values estimated compare well with those already reported in the literature.

Keywords

Calorimeters, kinetics constants, heat of reaction, activation energy, parameter estimation

Introduction

Isothermal reaction calorimeters are regularly used in the pharmaceutical and fine chemical industries to measure the reaction enthalpy and heat release rate (i.e., power) of a new chemical process under normal operating condition (Roberge, 2004). To simulate abnormal conditions, such as loss of cooling or an external fire, adiabatic calorimeters can be used to predict the runaway behavior of the reaction mixture. The knowledge gained from these studies enables the principles of inherently safer process design and safe operation to be built into the process conditions selected.

As the name suggests, in an isothermal calorimeter, the reaction mixture is maintained at a constant temperature by controlling the rate of heat exchange with the surroundings; these are usually in the form of an oil-filled heating/cooling jacket. They can be operated in either batch or semi-batch mode. In a batch calorimeter, all reactants are initially charged into the reactor vessel and subsequently only energy is allowed to cross the system boundaries. A semi-batch calorimeter usually involves two or more reaction components with the reactor being charged initially with one, or a combination, of the reactants, and then a final limiting reactant is gradually added over a period of time. The semi-batch mode of operation is often adopted to limit the accumulation of unreacted chemicals and hence the runaway reaction potential; it can also be used to suppress unwanted side reactions of higher order in the limiting reactant (Waldram, 1992).

The principal components of the isothermal calorimeter consist of the reactor vessel and a surrounding jacket with a circulating liquid that supplies heating or cooling to the reactor vessel, as shown in Figure 1. In addition, the reactor vessel also contains an electrical heater. This may be used to supplement the oil heating if a rapid heat-up rate is required, for calibrating the calorimeter or for heating at a variable rate if the power compensation method of calorimetry is being used. By using different measurement and control strategies, some calorimeters can be used in either the heat-flow or power-compensation modes (Zogg, et al., 2004).

Clearly, an isothermal calorimeter can play a vital role in determining the enthalpy of reaction and heat release rate of the chemical reaction(s). Moreover, by interpreting the temporal power curve, much can be learned about the kinetics of a given reaction. This type of analysis has been reported in the literature (Evans & Frey, 1980; Landau, et al., 1994; Landau 1996; Waldram, 1993; Zogg et al., 2004); however, the descriptions of the theoretical models used to estimate the kinetic parameters is limited. In this study, we have derived expressions for an isothermal calorimeter (operated in either the batch or semi-batch mode) that enable kinetic information to be extracted from the time varying reaction power curve. This extraction is possible since the instantaneous power, q_p , required to maintain the reactants at isothermal conditions is related directly to the rate at which new molecules are being formed by the reaction. Con-

Subramanya Nayak, Ph.D., is a senior scientist I at Abbott Laboratories. Before joining Abbott Laboratories, he was a post-doctoral associate in the chemical engineering department at Texas A&M University at Qatar and a research scientist in the Mary Kay O'Connor Process Safety Center at Texas A&M University. He can be contacted at subramanya.v.nayak@gmail.com.

M. Sam Mannan, Ph.D., is regents professor of chemical engineering and director of the Mary Kay O'Connor Process Safety Center at Texas A&M University. He can be contacted at manna@tamu.edu.

Simon Waldram, Ph.D., is a managing director at Waldram Consultants Ltd. and visiting scholar in the Mary Kay O'Connor Process Safety Center at Texas A&M University. Before joining Waldram Consultants Ltd., he was a professor and latterly interim program chair in the chemical engineering department at Texas A&M University at Qatar. He can be contacted at waldram@blueyonder.co.uk.

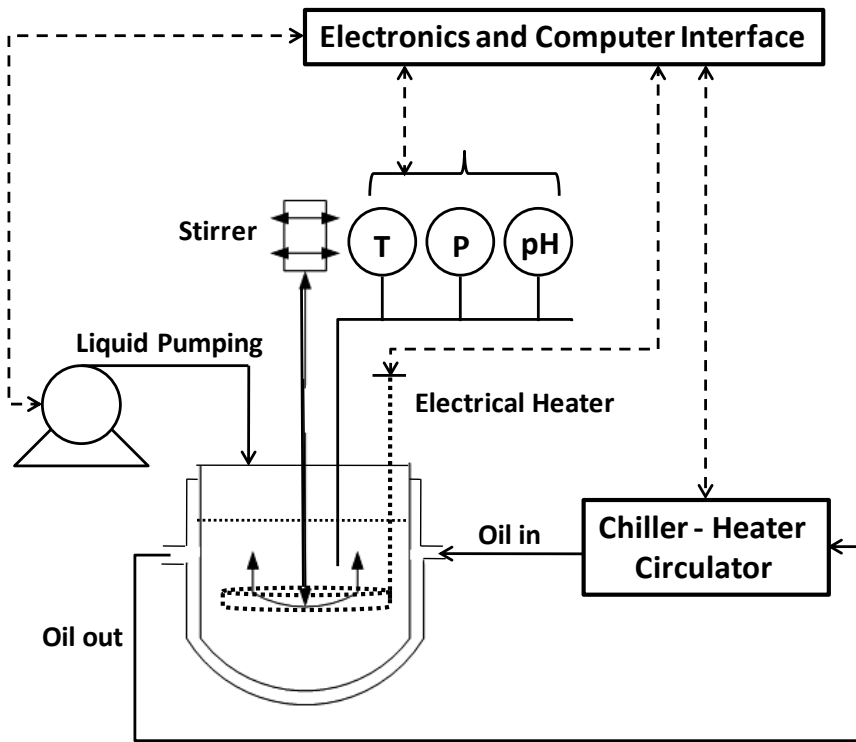


Figure 1. Principal components of an isothermal calorimeter.

sequently, for an n^{th} order kinetic model, q_r can be processed to estimate the order of the reaction, frequency factor and activation energy. To demonstrate the ability of the derived models to estimate kinetic constants, in the following section these are applied to the hydrolysis of acetic anhydride. The experiments were carried out at different temperatures in SIMULAR, an isothermal calorimeter manufactured by HEL Ltd. The estimates of the kinetic constants and activation energy are compared with published values in the open literature.

Isothermal Batch Calorimeter

As mentioned, in an isothermal batch calorimeter, no mass is added to, or removed from, the calorimeter during the reaction period. For example, for a single n^{th} order irreversible, exothermic reaction, only the power (q_r) generated is removed from the calorimeter, either by lowering the jacket temperature (heat flow calorimetry) or by reducing the power supplied to the electrical heater (power compensation calorimetry) so as to maintain the reaction mixture at isothermal conditions. The measured value of q_r can be related to the rate of reaction by means of equation (1):

$$q_r = -r_A (-\Delta H_r) V = k C_A^n (-\Delta H_r) V \quad (1)$$

and at any time t to C_A via equation (2):

$$C_A = \frac{Q_T - \int_0^t q_r dt}{Q_T} C_{A0} = [1 - x_A] C_{A0} \quad (2)$$

Here, x_A is fractional conversion defined as:

$$x_A = \frac{\int_0^t q_r dt}{Q_T}$$

Q_T is the total energy released during the course of the complete reaction (i.e. by definition):

$$Q_T = \int_0^\infty q_r dt$$

The heat of the reaction ($-\Delta H_r$) is calculated independently from the total energy exchange and is given as:

$$(-\Delta H_r) = \frac{Q_T}{C_{A0} V} = \frac{Q_T M w_A}{m_A} \quad (3)$$

Here, C_{A0} is the initial concentration of the reactant A , which is assumed to be totally consumed at the end of the batch reaction. V is the volume of the reaction mixture, and m_A is the mass of reactant A . This equation can readily be modified to apply to the situation where the

final concentration of species A does not fall to zero.

In equation (3), it is assumed that the heat of reaction is the overall averaged heat of reaction and that it is independent of conversion. Also, in equations (1) to (3), we assume that the volume of the reaction mixture remains constant. For most batch liquid phase systems, this assumption is reasonable. However, there are some cases, such as, polymerization, and gas phase reactions where volume, or density, varies significantly as a function of conversion. For these cases, one needs to account for volume change in analogous equations. The simplest assumption that can be made is that the volume (or density) varies linearly with conversion, i.e., $V = V_0(1 + \epsilon_A x_A)$, where ϵ_A is the fractional change in volume of the reaction mixture between zero and complete conversion (Levenspiel, 1999).

Combining equations (1) to (3) we get:

$$q_r = k C_{A0}^{(n-1)} [1 - x_A]^n Q_T \quad (4)$$

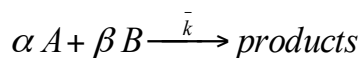
This expression can be used to represent q_r as a function of conversion to estimate the kinetic constant, k and order of the reaction, n . Either linear or nonlinear regression can be used to estimate these constants. In the linear form, equation (4) can be rewritten as:

$$\ln(q_r) = \ln(k Q_T C_{A0}^{(n-1)}) + n \ln[1 - x_A] \quad (5)$$

As a result, a plot of $\ln(q_r)$ vs. $\ln[1 - x_A]$ should yield a straight line with a slope equal to n and intercept equal to $\ln(k Q_T C_{A0}^{(n-1)})$ since n , C_{A0} and Q_T are already known, k can be evaluated. The temperature dependency of the kinetic constant can be then evaluated by performing a sequence of isothermal

calorimetry experiments at different temperatures and following the procedure explained earlier.

Now let us look at more complex reactions where two or more components are involved. For example:



and the reaction rate is given as:

$$-r_A = \frac{dC_A}{dt} = \bar{k} C_A^a C_B^b \quad (6)$$

Here, a is the order with respect to reactant A and b is the order with respect to reactant B . If $a = \alpha$ and $b = \beta$ then the reaction is "elementary" (i.e., the kinetics are of the order implied by the stoichiometry, but this is not necessarily so). If the reactants are mixed in their stoichiometric ratios, they will remain at that ratio throughout the reaction. Thus, the following will be true all of the time:

$$\frac{C_A}{C_B} = \frac{\alpha}{\beta} \quad (7)$$

Hence, the reaction rate in equation (6) can be rewritten as:

$$-r_A = \frac{dC_A}{dt} = \bar{k} \left[\frac{\alpha}{\beta} \right]^b C_A^{(a+b)} \quad (8)$$

If we combine $\bar{k} \left[\frac{\alpha}{\beta} \right]^b$ and represent it as k and $(a + b)$ as n , then equation (8) reduces to general n^{th} order kinetics and the approach discussed earlier in equation (4) can be applied to estimate the kinetic constant \bar{k} and order n . Separate experiments with a large excess of either reactant A or B will yield pseudo a^{th} or pseudo b^{th} order kinetics and the ability to estimate a and b individually.

In addition, the Half-Life ($t_{1/2}$) method to determine the overall reaction order and kinetic constant documented in standard texts, such as Levenspiel (1999) and Scott Fogler (2006), also can be used to analyze the temporal power curve. By definition, the half-life $t_{1/2}$ of the reaction is the time needed for the concentration of a key reactant to drop to one-half its original value. Thus, for an n^{th} order reaction:

$$t_{1/2} = \frac{(0.5)^{1-n} - 1}{k(n-1)} C_{A0}^{1-n} \quad (9)$$

or in the linear form:

$$\ln(t_{1/2}) = \ln \left[\frac{(0.5)^{1-n} - 1}{k(n-1)} \right] + (1-n) \ln(C_{A0}) \quad (10)$$

Referring to equation (2) we can relate $t_{1/2}$ to q_r as follows:

$$0.5 = 1 - \frac{\int_0^{t_{1/2}} q_r dt}{Q_T} \quad (11)$$

or,

$$\int_0^{t_{1/2}} q_r dt = \frac{Q_T}{2} \quad (12)$$

The value of t from the temporal power curve, which satisfies equation (12), is the value of $t_{1/2}$ for that particular species and initial concentration. If a series of experiments made with different initial concentrations indicate that $t_{1/2}$ is independent of C_{A0} , then the reaction order is one. If $t_{1/2}$ decreases as C_{A0} is increased, the reaction order is greater than unity whereas, if $t_{1/2}$ increases with C_{A0} , then the reaction order is less than unity. Equations (9) or (10) also can be applied to relate the values of C_{A0} with $t_{1/2}$ and hence to estimate n and k .

Note that all of this is only applicable for a single chemical reaction. If multiple chemical reactions are involved, additional information, such as reaction enthalpies and concentration of the products, will be required to decouple the instantaneous power curve and to estimate individual kinetic parameters.

Isothermal Semi-Batch Calorimeter

As mentioned, in an isothermal semi-batch calorimeter, reactant mass is added to the reactor during the reaction progress. Generally in semi-batch mode, the reactor vessel is initially filled with one reactant or a mixture of reactants with initial volume V_0 . At $t = 0$ the limiting reactant, say species A , is gradually pumped into the reactor at a constant volumetric flow rate v : in general, this results in a time varying concentration C_A of species A in the reactor. From the overall mass balance for a constant density system, we can calculate the total volume of the reacting mixture in the reactor at any time as:

$$V = V_0 + vt \quad (13)$$

and provided that no species A was added prior to $t = 0$, the concentration of reactant A is given as:

$$C_A = \frac{C_{A0} vt (1 - x_A)}{V} \quad (14)$$

Following the analogous reasoning to that for the isothermal batch calorimeter, the following expression defines the fractional conversion of species A :

$$x_A = \frac{\int_0^t q_r dt}{C_{A0} vt (-\Delta H_r)} \quad (15)$$

Here the numerator is the total heat produced up to time t , and the denominator is total heat produced if all A fed up to time t had reacted completely. Equations (13) to (15) are only applicable until the time when addition of reactant A ceases, after which the equations derived for the isothermal batch calorimeter become applicable. If the reaction is essentially instantaneous, q_r will always be equal to $C_{A0}v(-\Delta H_r)$, and the fractional conversion will always be unity (i.e., species A will be consumed essentially as soon as it enters the reactor).

For this particular case, note that the rate of reaction is feed rate limited rather than being controlled by the intrinsic chemical kinetics; thus, there can be no prospect of evaluating an order of reaction, kinetic constants or an activation energy from such an experiment, and the power generated by the reaction will be constant. If cooling is lost, and the feed is instantaneously isolated, then there will be no potential for a runaway reaction.

For an n^{th} order reaction:

$$q_r = k C_A^n (-\Delta H_r) V. \quad (16)$$

Combining equations (14) and (16) we get,

$$\frac{q_r}{V} = k (-\Delta H_r) \left[\frac{C_{A0} v t}{V} (1 - x_A) \right]^n, \quad (17)$$

or in the linear form

$$\ln\left(\frac{q_r}{V}\right) = \ln(k (-\Delta H_r)) + n \ln\left[\frac{C_{A0} v t}{V} (1 - x_A)\right]. \quad (18)$$

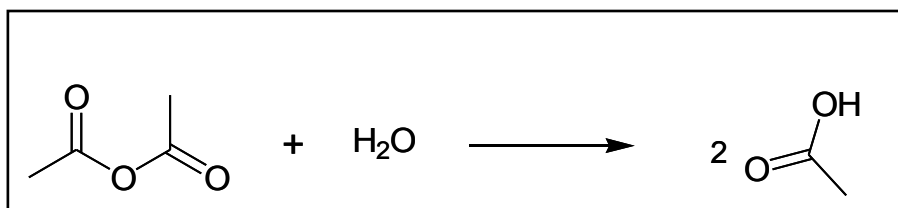
Either the linear or nonlinear form of equation (17) can be used to represent the semi-batch calorimetry data and to extract the relevant kinetic information.

Repeating the experiment over a range of temperatures will also enable the temperature dependency of the constants to be evaluated. As mentioned, the theoretical analysis presented in this section is only valid while reactant A is being added to the reactor. After the addition of reactant A ceases, the remaining power measured by the calorimeter is purely due to the batch mode of operation, and the analysis described in the preceding section should be applied. Note that in this case, the reactant concentrations within the reactor at the time when addition of the reactant A ceases must be used as the initial conditions for the batch operation.

As an illustration, hydrolysis of acetic anhydride has been studied in the HEL SIMULAR isothermal calorimeter. Some of the mathematical models derived in the preceding sections are applied to the experimental power measurements and the kinetic information is extracted. This analysis is explained in detail in the following section.

Hydrolysis of Acetic Anhydride

The overall hydrolysis reaction of acetic anhydride can be represented at right:



In an ideal batch reactor where we assume that the composition is uniform throughout the batch reactor at any instant of time, the rate of disappearance of acetic anhydride is given as:

$$-r_{(CH_3CO)_2O} = k [H_2O] [(CH_3CO)_2O]. \quad (19)$$

The reaction is first order with respect to both water and acetic anhydride (Hirota, et al., 2010). However, when a large excess of water is used, we can assume the reaction rate to be pseudo first order in acetic anhydride since the overall concentration of water hardly changes during the reaction (Kralj, 2007). Consequently, the rate of disappearance of acetic anhydride can be written as:

$$-r_{(CH_3CO)_2O} = k' [(CH_3CO)_2O]. \quad (20)$$

Here, k' is the pseudo kinetic constant defined as $k' = k[H_2O]$.

Experimental Section

In this study, we performed the hydrolysis reaction with a large excess of water. For reference, in all experiments, the minimum molar and volume ratios of water and acetic anhydride inside the reactor were 79:1 and 15:1, respectively. The experiments were performed at four different temperatures of 77 °F, 86 °F, 95 °F and 104 °F. The one-liter glass reactor was initially filled with 600 ml of deionized water and was set to reach a desired temperature. Once thermally stable, the fresh, commercial-grade acetic anhydride (99% by volume) was added into the reactor at a flow rate of 2.5 ml/min for 16 minutes. The reaction was then allowed to proceed until all acetic anhydride was consumed. Power-compensation calorimetry was used to determine the instantaneous power released by the hydrolysis reaction. In the power-compensation mode, the temperature difference between the reaction mixture and the circulating oil is always kept constant, and the power input to the electrical heater is varied to maintain the reaction mixture at an isothermal condition. Thus, during the exothermic hydrolysis reaction, the reactants were kept at constant temperature by reducing the power input to the electrical heater. Providing any net heating or cooling effect due to a difference between the feed (“dosing”) and reactor temperatures is taken into account; this reduction in supplied electrical power is a direct measurement of the power generated by the hydrolysis reaction. Consequently, no calibration was required.

Results & Discussion

Figure 2 shows the instantaneous power (q_r) generated by the hydrolysis reaction and the volume of acetic anhydride added to the reactor as function of time. The reaction was at 77 °F. The

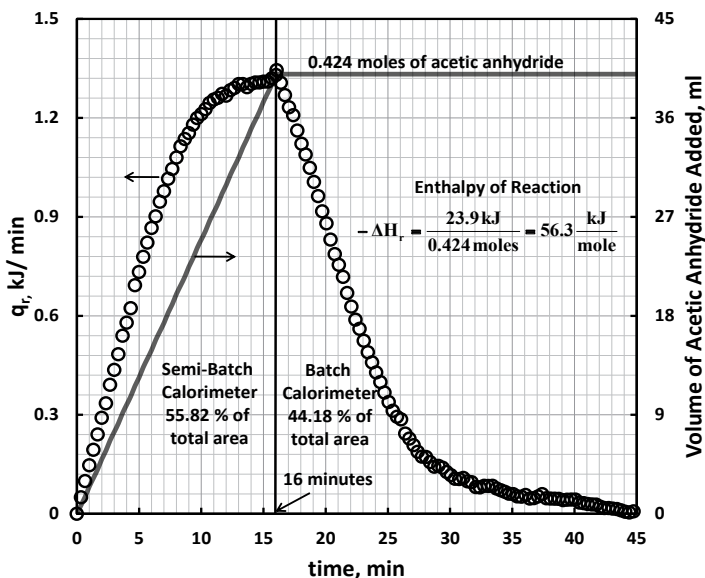


Figure 2. Illustration of the instantaneous power (q_r) measured by the SIMULAR calorimeter for the hydrolysis reaction performed at 77 °F, and the cumulative volume of acetic anhydride added to the reactor as a function of time.

enthalpy of the hydrolysis reaction was calculated by dividing the total area under the q_r vs t curve by the total moles of acetic anhydride added into the reactor. It was found that $-\Delta H_r = 56.25$ kJ/mole exothermic. This value compares well with the values of 56.0 and 58.2 kJ/mole reported in the literature (Haji & Erkey, 2005; Kralj, 2007). The initial part of the temporal q curve, until $t = 16$ corresponds to the semi-batch mode of the operation and the remaining part to the batch mode of operation, as illustrated in Figure 2. Consequently, to estimate the kinetic constant for the pseudo first order hydrolysis reaction, these curves should be treated using their respective mathematical equations described in the previous sections.

The nonlinear behavior of the curve observed in Figure 2 was expected since under the experimental conditions chosen, the rate of reaction was kinetically limited. Initially, when acetic anhydride is added to the reactor, it does not react instantaneously. Some of it accumulates and gradually reacts with time on stream. This explains the initial steep rise in the temporal curve and then the gradual decline in the slope of the curve during the semi-batch mode of operation. The reason for observing the small “bump” at the end of dosing is due to the fact that the electrical heater must adjust to the cessation of the cooling effect associated with dosing feed that is at a lower temperature than the reaction mixture.

Figure 3 shows the best fit between the experimental and modeled temporal q curves at 77 °F. A nonlinear least squares method was used to minimize the differences between the experimental and modeled values. As mentioned, the initial part of the temporal q curve up to $t = 16$ was treated as from a semi-batch reactor, and equation (17) was used to estimate the kinetic constant. After 16 minutes, the data were from a batch reactor, and equation 4 was used to estimate the kinetic constant.

In Figure 3, it can be observed that the optimum value of k' enables predictions from the equations to be reconciled

closely with the experimental data. This match helps justify the assumptions used when developing both the batch and semi-batch isothermal calorimeter models. The values of k' estimated in this study and in the literature (Haji & Erkey, 2005) are presented in Table 1: good agreement is observed. This confirms the validity of evaluating kinetic parameters from conventional calorimetry data (rather than from samples) in the manner described in this paper.

The temperature dependency of the estimated pseudo kinetic constant is represented by the Arrhenius equation,

$$k' = k'_o \exp\left(\frac{-E_a}{RT}\right) \quad (21)$$

Table 2 reports the estimated activation energy, E_a from this study based on 4 isothermal experiments (conducted at 77 °F, 86 °F, 95 °F and 104 °F) and from the literature (Asprey, et al., 1996; Haji & Erkey, 2005; Kralj, 2007; Shatynski & Hanesian, 1993). It is found that the calculated activation energy falls within the range of values reported in the literature.

Summary

We have developed some simple theoretical models to estimate kinetic constants by interpreting the temporal instantaneous power curve generated from a single chemical reaction experiment in an isothermal calorimeter. The models derived in this study are capable of interpreting data gathered during both batch and semi-batch modes of operation. The ability to use these models to estimate kinetic constants and their temperature dependency was tested. The hydrolysis reaction of acetic anhydride was performed in the HEL SIMULAR reaction calorimeter. It is shown that the estimates of the kinetic constants and activation energy for this hydrolysis reaction match well with values reported in the literature. Importantly,

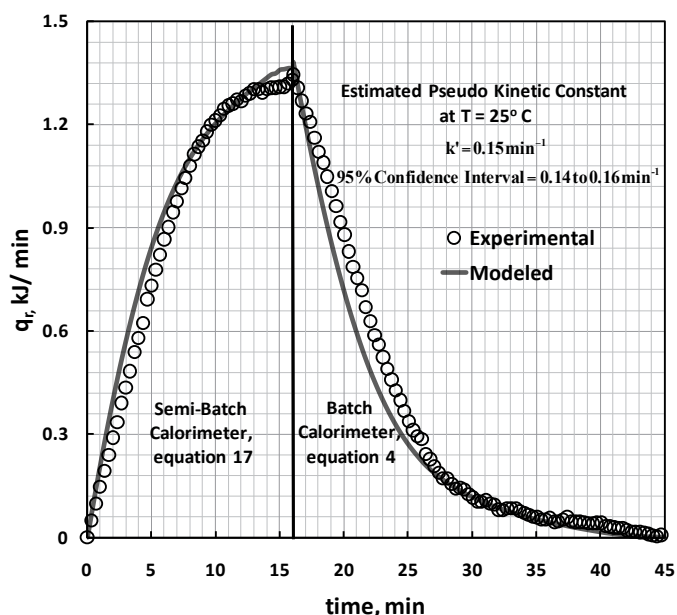


Figure 3. Experimental and modeled temporal curves at 77 °F.

the method presented here requires no additional sampling or analysis of the reaction mixtures. However, additional sampling and analysis are recommended, and may be essential, especially when multiple reactions are involved or when dealing with complex phenomena, such as mass transfer limitations, multiphase flows and phase change.

We believe that the type of theoretical analysis presented in this study can be of tremendous help during the initial stage of process development and modeling of potential reactor performance. The ability to choose reactant concentrations, operating temperature and semi-batch addition time so as to minimize the potential for a runaway exothermic reaction can be simulated using parameters derived in the manner described here. Predictions can then be confirmed by further adiabatic experiments. In this manner, a move toward inherent safety can be built into the process development. ☉

Nomenclature

a, b	reaction orders for components A and B
α, β	stoichiometric coefficients for components A and B
C_{A0}	initial concentration of the reactant, mole/m ³
C_A	concentration of the reactant, mole/m ³
E_a	activation energy, kJ/mole
k, \bar{k}	kinetic constant, (mole/m ³) ⁿ .s ⁻¹
k'_o	pre-Arrhenius factor, equation 21, (mole/m ³) ⁿ .s ⁻¹
k'	pseudo first order kinetic constant, s ⁻¹
m_A	mass of reactant A, gm
Mw_A	molecular weight of reactant A, gm
n	order of the reaction
q_r	instantaneous power, kJ/s
Q_T	total energy released, kJ
$-r_A$	reaction rate, (mole/m ³).s ⁻¹
R	ideal gas constant, (kJ/(mole.K))
t	time, s

$t_{1/2}$	half-life of the reaction, s
V	volume of the reaction mixture, m ³
V_0	initial volume of the reaction mixture, m ³
v	volumetric flow rate, m ³ /s
x_A	fractional conversion of reactant A
ΔH_r	heat of the reaction, kJ/mole
ε_A	fraction volume change

References

- Asprey, S., Wojciechowski, B., Rice, N. & Dorcas, A. (1996). Applications of temperature scanning in kinetic investigations: The hydrolysis of acetic anhydride. *Chemical Engineering Science*, 51(20), 4681-4692.
- Evans, F.W. & Frey, H. (1980). Reaction kinetics from calorimetric studies. *Chimia: International Journal of Chemistry*, 34(50), 247-252.
- Haji, S. & Erkey, C. (2005). Kinetics of hydrolysis of acetic anhydride by in situ FTIR spectroscopy. *Chemical Engineering Education*, (Winter), 56-61.
- Hirota, W., Rodrigues, R., Sayer, C. & Giudici, R. (2010). Hydrolysis of acetic anhydride: Non-adiabatic calorimetric determination of kinetics and heat exchange. *Chemical Engineering Science*, 65, 3849-3858.
- Kralj, A. (2007). Checking the kinetics of acetic acid production by measuring the conductivity. *Industrial & Engineering Chemistry Research*, 13(4), 631-636.
- Landau, R.N., Blackmond, S.G. & Tung, H.H. (1994). A calorimetric investigation of an exothermic reaction: Kinetic and heat flow modeling. *Industrial & Engineering Chemistry Research*, 33(4), 814-820.
- Landau, R.N. (1996). Expanding the role of reaction calorimetry. *Thermochimica Acta*, 289(2), 101-126.
- Levenspiel, O. (1999). *Chemical reaction engineering* (3rd ed.). New York: Wiley.
- Roberge, D. (2004). An integrated approach combining reaction engineering and design of experiments for optimizing reactions. *Organic Process Research & Development*, 8(6), 1049-1053.
- Scott Fogler, H. (2006). *Elements of chemical reaction engineering* (4th ed.). New Jersey: Prentice-Hall.
- Shatynski, J. & Hanesian, D. (1993). Adiabatic kinetics studies of the cytidine/acetic anhydride reaction by utilizing temperature versus time data. *Industrial & Engineering Chemistry Research*, 32(4), 594-600.
- Waldram, S. (1992). Semi-batch exothermic reaction processing, a move toward inherent safety. *Chemical Industry Digest (India)*, 3rd Qtr., 3, 135-141.
- Waldram, S. (1993). Isothermal calorimetry: Extracting kinetic information from heat flux measurements. *Chemical Industry Digest (India) 1st Qtr.*, 1, 111-114.
- Zogg A., Stoessel, F., Ulrich, F. & Hungerbuhler, K. (2004). Isothermal reaction calorimetry as a tool for kinetic analysis. *Thermochimica Acta*, 419(1-2), 1-17.

Temperature, °F	This study, k' , min ⁻¹	95% Confidence Interval, min ⁻¹	Haji & Erkey (2005) k' , min ⁻¹
77	0.15	0.14 to 0.16	0.158
86	0.24	0.22 to 0.26	
95	0.29	0.27 to 0.31	0.275
104	0.38	0.37 to 0.40	

Table 1. The values of the kinetic constant, k' for the pseudo first order hydrolysis of acetic anhydride with water at different temperatures.

Reference	Measuring Technique	E_a , kJ/mole
This study	Isothermal Calorimeter	47.1
Shatynski & Hanesian (1993)	Adiabatic Calorimeter	46.9
Asprey, et al., (1996)	Conductivity	45.7
Kralj (2007)	Conductivity	50.1
Haji & Erkey (2005)	FTIR	53.6

Table 2. Values of activation energy E_a for the hydrolysis reaction.

Acknowledgment

The authors would like to thank the Qatar Foundation and Texas A&M University at Qatar for financial support for these studies.

Acknowledgment of Reviewers

The *Journal of Safety, Health and Environmental Research* gratefully acknowledges the following individuals for their time and efforts as manuscript reviewers during the period between Sept. 1, 2011, and Aug. 31, 2012. Their assistance in raising the standard of the papers published is immense and is greatly appreciated. Although the members of the Editorial Review Board (names are italicized) generally reviewed more manuscripts than others (and provided much additional support), the vast majority of reviews were handled by ad hoc reviewers, chosen for their unique expertise on the topics under consideration.

Magdy Akladios, University of Houston-Clear Lake, Houston, TX, USA

Alex Albert, University of Colorado, Boulder, CO, USA

Ammar Alkhalaf, Texas A&M University, College Station, TX, USA

Earl Blair, Indiana University, Bloomington, IN, USA

James Borchardt, Bettendorf, IA, USA

David Borys, University of Ballarat, Ballarat, Victoria, Australia

Sang Choi, University of Wisconsin-Whitewater, Whitewater, WI, USA

John Culvenor, University of Ballarat, Ballarat, Victoria, Australia

Jerry Davis, Auburn University, Auburn, AL, USA

Angela DiDomenico, Liberty Mutual Research Institute for Safety, Hopkinton, MA, USA

Lon Ferguson, Indiana University of Pennsylvania, Indiana, PA, USA

Yang Miang Goh, National University of Singapore (NUS), Singapore

Jon Ivar Håvold, Aalesund University College, Aalesund, Norway

Taesik Lee, Korea Advanced Institute of Science and Technology (KAIST), South Korea

Marc Levin, Shell Canada Ltd., Calgary, Alberta, Canada
Ciaran McAleenan, University of Ulster, Jordanstown, Northern Ireland, U.K.

Michael O'Toole, Embry-Riddle Aeronautical University, Daytona Beach, FL, USA

Maria Papadaki, University of West Greece, Agrinio, Greece

Hans Pasman, Delft University of Technology, Delft, The Netherlands

Sathy Rajendran, Central Washington University, Ellensburg, WA, USA

Sanjeev Saraf, Exponent, Houston, TX, USA

Richard Sesek, Auburn University, Auburn, AL, USA

Paul Specht, Millersville University, Millersville, PA, USA

Anthony Veltri, Oregon State University, Corvallis, OR, USA

Donna Vosburgh, University of Wisconsin-Whitewater, Whitewater, WI, USA

Sam Wamuziri, Glyndwr University, Wales, U.K.

Qingsheng Wang, Oklahoma State University, Stillwater, OK, USA

Cindy Wei, BASF Corporation, Wyandotte, MI, USA

Steven Zhang, Mustang Engineering, Houston, TX, USA ☉